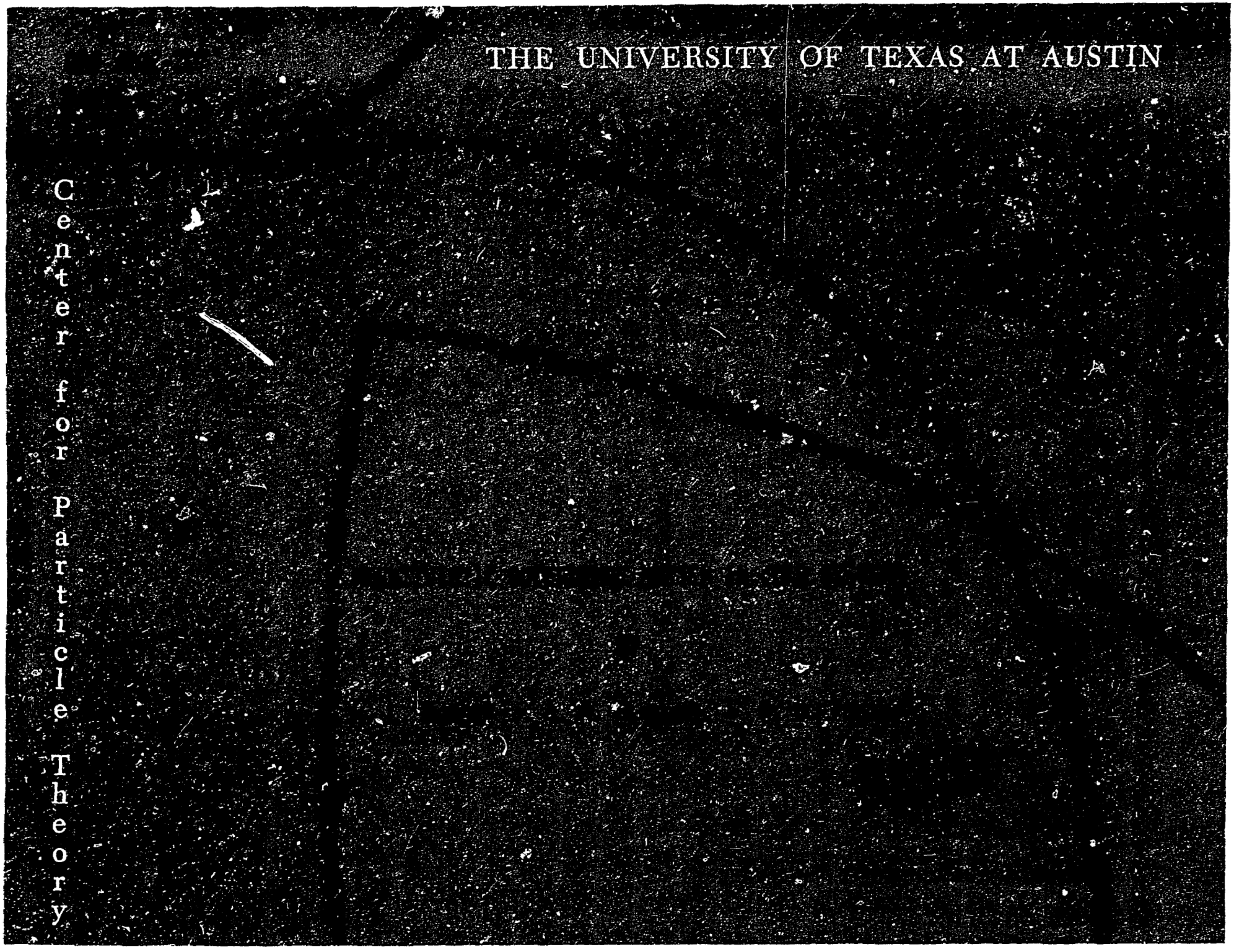

ORO-3992-207
CPT 251

Relativistic Superdense Matter in Cold Systems†

Richard L. Bowers

Department of Physics
Texas A & M University
College Station, Texas

and

A. M. Gleeson and R. Daryl Pedigo

Center for Particle Theory
Physics Department
University of Texas at Austin
Austin, Texas

†Work supported by the U. S. Atomic Energy Commission, Contract No. AT(40-1)3992.

Abstract

A fully relativistic model of the strong interactions between hyperons, fitted to nuclear matter, is used to investigate the properties of superdense matter. This model can be solved exactly, and the low temperature limit applied directly to construct neutron star models. Our results predict a significantly higher mass stability limit ($M_{max} = 2.39M_{\odot}$) which has far-reaching implications for black hole astrophysics. It also predicts moments of inertia well above the observational lower bounds for pulsars. The model predicts a phase transition which includes nuclear densities, and has significant implications for the detailed structure of neutron stars. Despite the low central densities found for stable masses ($\epsilon_c \leq 2 \times 10^{15} g/cm^3$) all members of the first SU(3) symmetric octet except the Ξ^- enter as stable constituents.

In addition, quarks may be used as fundamental constituents for a species of superdense matter applicable to models of the hyperons. Our results indicate that this approach may be fruitful in explaining such phenomena as precocious scaling and quark confinement.

I. Introduction

The observation of exotic astrophysical phenomena during the last decade has stimulated an interest in the investigation of matter under extreme conditions. In this paper we study what is commonly called superdense matter.[1] These are the states of matter which occur near the limit of gravitational collapse. We are particularly interested in superdense matter in neutron stars because they play a central role in current models of pulsars and compact x-ray sources in binary systems. In addition, we mention briefly the application of this kind of matter to models of elementary particles.

A general feature shared by all previous models of neutron stars is that the more massive have average core densities greater than 10^{15}g/cm^3. With few exceptions these models all predict stars with masses less than $1.4M_\odot$ to $1.76M_\odot$. These models are developed from non-relativistic theories and are based on our understanding of the properties of nuclear matter.[1,2] A disturbing feature of this situation is that the high mass models involve densities which are above nuclear density where relativistic effects are significant and cannot be ignored. It is therefore necessary to approach the problem from a fully relativistic interacting many-body theory.

In this paper we report the results of a study of superdense matter based on a fully relativistic phenomenological description of the strong interactions. The strengths of these interactions are determined by a fit to nuclear matter. These are then employed within the framework of a many-body theory, which is also relativistic, to calculate baryon composition and the pressure-energy density equation of state for stellar matter. The relativistic stellar structure equations at T=0 are then integrated using this equation of state.

The predictions of this model differ significantly from previously described results,[2] and stand in more satisfactory agreement with current evolutionary predictions and observational limits. The stability limit against gravitational collapse is $2.39M_\odot$. This higher mass limit is particularly important since it implies that black hole formation may be less frequent than current theories of superdense matter suggest. The moments of inertia for intermediate and high mass stars ($\gtrsim 10^{45}$g/cm^3) bring models of pulsars as rapidly rotating neutron stars well within the limits set by observations.[3,4] Finally we note that our model leads to a picture of compact object formation which is in general accord with the results of evolutionary studies.[5]

The results of our investigations will be discussed in the following order. In Section II we use a phenomenological lagrangian to explore the properties of strongly interacting superdense matter in Born approximation. This approach, which is found to be inadequate, leads to the consideration of an expansion in density rather than in the coupling constants. This expansion in density then motivates construction of an effective lagrangian which retains the major features of the strong interactions for densities relevant to neutron stars. This construction is given in Section III. From this lagrangian we obtain relativistic finite density Green's functions. These are used to obtain expressions for the baryon effective masses, and self-consistency conditions on the baryon number and proper number densities. In Section IV we derive expressions for the chemical potentials, pressure, energy density and speed of sound. We then fix the coupling constants by fitting the model to nuclear matter. A numerical solution of these quantities, including a phase transition in the vicinity of nuclear density, is presented in Section V. In Section VI we consider corrections to the chemical potentials and effective masses due to finite temperature effects in the high density, low temperature limit. Our T=0 results are then used in Section VII to construct neutron star models. The relation between our results

and the implications of evolutionary studies and observational limits are discussed. In Section VIII we consider the expected effects of non-normal ground states. Also discussed are the limitations of the model and its possible application to models of elementary particles.

Throughout our discussions we have set $\hbar = c = 1$.[6]

II. Fundamental Interactions

In a field theoretic approach to many-body theory the boundary conditions which reflect the finite density and temperature of the system are most naturally incorporated through the use of Green's functions. The relativistic formulation of this problem has already been discussed.[7,8]

It is natural, in formulating a model of superdense matter, to try to include a large fraction of the known particles and resonances as possible constituents. A reasonable trial group might include the first SU(3) symmetric octet of baryons, the electron and muon, and low-lying mesons. Adopting these as fundamental fields, the system can be described by the lagrangian density

$$\mathcal{L}(x) = \sum_B \bar{\psi}_B(x)(i\not{\partial}-m_B)\psi_B(x) + \sum_L \bar{\psi}_L(x)(i\not{\partial}-m_L)\psi_L(x) + \sum_P \mathcal{L}_P + \mathcal{L}_I + \mathcal{L}_C. \qquad (2.1)$$

Baryons are denoted by B, leptons by L and mesons by P. $\mathcal{L}_C$ contains all mass counterterms, and the physical masses m_B and m_L are included in Table 1.

The term $\mathcal{L}_I$ represents the meson exchanges among the hadrons. In the density range of interest, $\varepsilon \sim 10^{14}$ g/cm^3 up to

$\sim 10^{16}$ g/cm^3, the important exchanged mesons are the π, η, ρ, ω, δ and ϕ. Because of charge constraints the presence of the leptons has an important effect on the relative concentrations of the other species, but their interactions with the baryons are negligible. The interaction term can then be written as

$$\mathcal{L}_I = \sum_{B,P} \bar{\psi}_B \Gamma_{BB'P} \psi_{B'} \phi_P g_{BB'P}. \qquad (2.2)$$

The $\Gamma_{BB'P}$ include pseudoscalar, scalar and vector couplings, and the strengths $g_{BB'P}$ may be fixed by requiring that (2.2) reproduce the nucleon-nucleon scattering data in the Born approximation.

The two point functions are defined in terms of the elementary fields by

$$G_F^{(B)}(x-x') = -i\langle T\psi_B(x)\bar{\psi}_B(x')\rangle \qquad (2.3)$$

and

$$D_F^{(P)}(x-x') = -i\langle T\phi_P(x)\phi_P(x')\rangle \qquad (2.4)$$

where the brackets denote a suitably defined relativistic thermodynamic average.[7] At zero temperature the latter is over the baryon N-body ground state, and T is the time ordering operator. The equations of motion for $D_F^{(P)}$ and $G_F^{(B)}$ which couple to higher order N-point functions are generated from (2.1) in the usual way. Approximations must be made if we are to solve these equations. One approach is to

solve the Green's function Dyson equations truncated to second order in perturbation theory.

The appearance of real mesons in the system would introduce complications. Being bosons, they may form condensates, which would require the incorporation of non-normal ground states. These effects may be included in our approach. However, as argued in Section VIII, their presence is not expected to alter the basic structure of neutron stars. We therefore set $L_p = 0$ in (2.1) and consider only virtual mesons, described by the usual vacuum propagators, in this calculation.

The non-interacting spin ½ baryon propagator corresponding to a finite density T = 0 system is

$$S_F(p,q_F) = \frac{\not{p}+m}{2E_p}\left\{\frac{1-n_F(\vec{p})}{p^0-E_p^{\rightarrow}+i\epsilon} + \frac{n_F(\vec{p})}{p^0-E_p^{\rightarrow}-i\epsilon} - \frac{1}{p^0+E_p^{\rightarrow}-i\epsilon}\right\}, \quad (2.5)$$

where $n_F(\vec{p})$ is the T=0 Fermi distribution step-function, and all other variables have their usual meaning.[7] The number of baryons N in a system of volume V is related to the Fermi wave vector by

$$3\pi^2 N/V = q_F^3. \quad (2.6)$$

Standard perturbation theory applied to a model of this kind leads to baryon self-energy diagrams such as those shown in Figure 1. Tadpole diagrams (Fig. 1a) vanish identically for the exchanged mesons discussed above, since a non-vacuum-valued quantum number is carried by each. To lowest order, the self-energy contains only bubble diagrams and $G_F^{(B)}(p,q_F)$ will be given by[9]

$$\{(\not{p}-\not{\Sigma}^{(B)}(p,q_F)) - (m_B+\Sigma^{(B)}(p,q_F))\}\, G_F^{(B)}(p,q_F) = 1 \quad (2.7)$$

where $\not{\Sigma}^{(B)}$ and $\Sigma^{(B)}$ contain a contribution from each of the exchanged mesons. In each of these self-energies we can uniquely separate out a finite density dependent part:

$$\not{\Sigma}^{(B)}(p,q_F) = \not{p}S_2^{(B)}(p^2) + \not{\Sigma}_f^{(3)}(p,q_F) \quad (2.8)$$

$$\Sigma^{(B)}(p,q_F) = m_B S_1^{(B)}(p^2) + \Sigma_f^{(B)}(p,q_F). \quad (2.9)$$

The terms S_1 and S_2 represent the elementary particle self-energy which survives at zero baryon density. These terms are divergent, and are renormalized by subtraction to the baryon physical mass. Although S_1 and S_2 are not explicitly density dependent, there is an implicit dependence, since they are sensitive to the value of p^2 which is driven off the mass shell by the density effects.

The excitation energies and chemical potentials of the baryons may be obtained from the poles of $G_F^{(B)}(p,q_F)$. In the interest of simplicity let us discuss the exchange of only one meson. We find that

$$G_{F\alpha\beta}^{(B)}(p,q_F) = \frac{N(p,q_F)_{\alpha\beta}}{D(p,q_F)} , \qquad (2.10)$$

where the denominator is given by

$$D(p,q_F) = \{p^0(1-S_2(p^2)) - \Sigma_f^0(p,q_F)\}^2$$

$$- \{|\vec{p}|(1-S_2(p^2))-\Sigma_f^v(p,q_F)\}^2-\{m_B(1+S_1(p^2))+\Sigma_f(p,q_F)\}^2. \qquad (2.11)$$

The term Σ_f^v represents the 3-vector magnitude of $\Sigma_f^\mu(\mu=1,2,3)$. The excitation energies $p^0 = p^0(q_F,p)$ are obtained as solutions of

$$D(p^0,\vec{p},q_F) = 0, \qquad (2.12)$$

and the chemical potential (equal to the Fermi energy at $T = 0$) is given by

$$\mu(q_F) = p^0(|\vec{p}| = q_F,q_F). \qquad (2.13)$$

The solutions of (2.12) for pseudoscalar, scalar, and vector mesons have been investigated numerically for densities $\lesssim (q_F/m_B \sim 1)$. Low density expansions have also been made for the region $q_F/m_B << 1$. We find generally that (a) the terms $S_i(p^2)$ are sensitive to deviations away from mass shell; (b) Σ_f^0, Σ_f^v and Σ_f, though strongly density dependent, beat against one another in such a way that their leading order contributions cancel.

For the dominant exchanges of π and ρ we found several additional features. For some range of the renormalized coupling constant $g_{\pi NN}$ a ghost develops and solutions to (2.12) are not found for real values of p^0. For sufficiently weak coupling solutions are found in the density range considered ($0.05 < q_F/m_N < 1.0$). The leading order terms in the π exchange model yield attractive nucleon-nucleon interactions. However, these terms cancel in (2.12), and the next order terms correspond to an effective increase in the value of p^0. In fact the chemical potential μ is greater than that of a free gas at the same density.[10] Analysis of ρ exchange leads to much the same conclusion: Leading order effects tend to cancel, and higher order terms yield a chemical potential for vector exchange which lies below a free gas, which is the opposite of the expected result of repulsion.

A model based on Born terms is clearly inadequate. At the very least we should retain terms representing fourth order processes (Figure 1c-1d) in a calculation of the Green's functions. Analysis of these terms for baryons

shows that they have leading order density dependence proportional to baryon number density. Furthermore in the density range of interest the dominant term in each is, to within a density independent factor, the same as the tadpole term (Figure 1a). In fact the finite N^{th} order contribution should also show a density dependence at most proportional to q_F^3 in this range.

These observations suggest that expansion in powers of the renormalized coupling constants should be replaced by an expansion in density as illustrated schematically in Figure 1e. The first term in this series is just the tadpole graph which was discarded previously. Moreover, this simple term is proportional to the leading order corrections from the higher order expressions in Figure 1e. Thus we approximate the interactions due to meson exchange in super-dense matter by expressions proportional to the primitive tadpole diagram represented in Figure 1a. The constants of proportionality may be determined phenomenologically. Since we treat only spin ½ baryons the only phenomenological fields of interest are the scalar and vector fields.

When the self-energy corresponding to Figure 1a is examined for these cases it is found to be repulsive for vector exchange. Scalar exchange produces attraction in the lower density region, but becomes repulsive at larger densities.

The system treated in this fashion thus enjoys all the expected behavior for the exchanges studied, and does not suffer from the difficulties of nearby ghost states with their associated anomalous properties.

III. Phenomenological Model

The analysis of the previous section suggests that we consider as a model of the strong interactions in superdense matter the baryons coupled via a vector and a scalar field which have vacuum quantum numbers. A universal SU(3) symmetric coupling will be assumed. The effective lagrangian density then has the form

$$\begin{aligned} L(x) &= \sum_B \bar{\psi}_B(x)(i\partial\!\!\!/ - m_B)\ \psi_B(x) \\ &\quad - \sum_B \{g_S \bar{\psi}_B(x)\psi_B(x)\phi_S(x) + g_V \bar{\psi}_B(x)\gamma_\mu \psi_B(x)\phi_V^\mu(x)\} \\ &\quad + \tfrac{1}{2}\{\partial_\mu \phi_S(x)\partial^\mu \phi_S(x) - \mu_S^2 \phi_S(x)^2\} - \tfrac{1}{2}F^{\mu\nu}(x)F(x)_{\mu\nu} \\ &\quad + \tfrac{1}{2}\mu_V^2 \phi_V^\nu(x)\phi_V(x)_\nu, \end{aligned} \tag{3.1}$$

where

$$F^{\mu\nu}(x) = \partial^\mu \phi_V^\nu(x) - \partial^\nu \phi_V^\mu(x). \tag{3.2}$$

The counter terms have been dropped since all expressions to be considered below are finite. Accordingly we understand m_B to represent the baryon physical masses.

A more appropriate effective lagrangian, which is consistent with our earlier statements about the non-observability of the meson degrees of freedom, should contain only

baryon fields. A non-local lagrangian, equivalent to the above, is

$$\begin{aligned} L(x) &= \sum_B \bar{\psi}_B(x)(i\partial\!\!\!/ - m_B)\ \psi_B(x) \\ &\quad - \sum_{BB'} \{\int d\xi\, g_S^2 \bar{\psi}_B(x)\psi_B(x)\Delta(x-\xi)\bar{\psi}_{B'}(\xi)\psi_{B'}(\xi) \\ &\quad + \int d\xi\, g_V^2 \bar{\psi}_B(x)\gamma_\mu \psi_B(x)\Delta^{\mu\nu}(x-\xi)\bar{\psi}_{B'}(\xi)\gamma_\nu \psi_{B'}(\xi)\}. \end{aligned} \tag{3.3}$$

The Δ's appearing in (3.3) are the time symmetric vacuum two-point functions for phenomenological scalar and vector fields. We thus retain the role of the mesons as mediating the interactions without allowing their presence as physical particles.[11] Functional variation of the thermodynamic average of this lagrangian yields the equations of motion for the baryon Green's functions. These are

$$\begin{aligned} (i\partial\!\!\!/ - m_B)G_F^{(B)}(x-x') &= -\delta(x-x') \\ &\quad + \sum_{B'} g_S^2 \int d^4\xi \Delta(x-\xi) G_F^{(BB')}(x\xi, x'\xi^-) \\ &\quad + \sum_{B'} g_V^2 \int d^4\xi \Delta_{\mu\nu}(x-\xi)\gamma^\mu G_F^{(BB')}(x\xi, x'\xi^-)\gamma^\nu, \end{aligned} \tag{3.4}$$

where we have defined the four-point function by

$$G_F^{(B\,B')}(xy, x'y') = (1/i)^2 \langle T\psi_B(x)\bar{\psi}_{B'}(y)\bar{\psi}_{B'}(y')\bar{\psi}_B(x')\rangle, \tag{3.5}$$

and the notation ξ^- signifies that the time component is infinitesimally earlier than ξ.

The Hartree-Fock approximation to (3.4) results if we set

$$G_F^{(BB')}(xy,x'y') = G_F^{(B)}(x-x')G_F^{(B')}(y-y') - G_F^{(B)}(x-y)G_F^{(B')}(y'-x')\delta_{BB'}. \quad (3.6)$$

The notation in the last term reflects the fact that the two-point functions are diagonal in baryon index. This term leads to self-energy contributions like the bubble diagram shown in Figure 1b, while the first term leads to tadpole diagrams (Figure 1a). Motivated by the discussion of the previous section, we retain the first or Hartree term in (3.6), since it represents the leading order correction in powers of the density. The resulting equations of motion become

$$(i\not{\partial} - m_B)G_F^{(B)}(x-x') = -\delta(x-x') + \sum_{B'}\{g_s^2\int d^4\xi\Delta(x-\xi)G_F^{(B')}(\xi-\xi^-) + g_v^2\int d^4\xi\Delta_{\mu\nu}(x-\xi)\gamma^\nu G_F^{(B')}(\xi-\xi^-)\gamma^\nu)G_F^{(B)}(x-x'). \quad (3.7)$$

A substantial simplification results if we consider (3.7) in momentum space. Using

$$G_F^{(B)}(x-x') = \int \frac{d^4p}{(2\pi)^4} e^{-ip\cdot(x-x')}G_F^{(B)}(p) \quad (3.8)$$

and

$$\Delta(x-x') = \int \frac{d^4k}{(2\pi)^4} e^{-ik\cdot(x-x')}\Delta(k) \quad (3.9)$$

for the scalar and vector propagators, it immediately follows that

$$(\not{p}-m_B)G_F^{(B)}(p,q_{FB},q_{F\alpha}) = 1 + \lim_{\eta\to 0^+}\sum_{B'}\Big\{-g_s^2/\mu_s^2\int\frac{d^4q}{(2\pi)^4}e^{iq^0\eta}\mathrm{tr}\left[G_F^{(B')}(q,q_{FB'},q_{F\alpha})\right] + \gamma^0 g_v^2/\mu_v^2\int\frac{d^4q}{(2\pi)^4}e^{iq^0\eta}\mathrm{tr}\left[\gamma^0 G_F^{(B')}(q,q_{FB'},q_{F\alpha})\right]\Big\}G_F^{(B)}(p,q_{FB},q_{F\alpha}). \quad (3.10)$$

The factors $-\mu_s^{-2}$ and $-\mu_v^{-2}$ are the $k^2 = 0$ scalar and vector propagators, and the traces over $G_F^{(B')}$ and $\gamma^0 G_F^{(B')}$ have been shown explicitly. The factors $e^{iq^0\eta}$ specify the integration contour in the q^0 plane, and result from the temporal constraint on ξ in (3.7). The density dependence of $G_F^{(B)}(p,q_{FB},q_{F\alpha})$ has been explicitly exhibited. It should be emphasized that each baryon Green's function depends on its density q_{FB} and, through the interactions, on the density of all other baryons actually present in the system. The latter are collectively denoted by $q_{F\alpha}$. The terms in brackets are the vector and scalar self-energies, which we denote by

$$\Sigma_s^{(BB')} = \frac{g_s^2}{\mu_s^2}\lim_{\eta\to 0^+}\int\frac{d^4q}{(2\pi)^4}e^{iq^0\eta}\mathrm{tr}\left[G_F^{(B')}(q)\right], \quad (3.11)$$

and

$$\Sigma_v^{(BB')} = \frac{g_v^2}{\mu_v^2}\lim_{\eta\to 0^+}\int\frac{d^4q}{(2\pi)^4}e^{iq^0\eta}\mathrm{tr}\left[\gamma^0 G_F^{(B')}(q)\right]. \quad (3.12)$$

In terms of $\Sigma_V^{(BB')}$ and $\Sigma_S^{(BB')}$ the Green's functions are given by

$$\{\not{p} - m_B - \sum_{B'} (\Sigma_S^{(BB')} + \gamma^0 \Sigma_V^{(BB')})\} G_F^{(B)}(p) = 1 . \quad (3.13)$$

The last equation may be inverted directly to obtain

$$G_F^{(B)}(p) = \frac{\gamma^0 (p^0 - \Sigma_V^{(B)}) - \vec{\gamma}\cdot\vec{p} + m_B + \Sigma_S^{(B)}}{[p^0 - \Sigma_V^{(B)}]^2 - p^2 - [m_B + \Sigma_S^{(B)}]^2} , \quad (3.14)$$

where the obvious notation $\Sigma^{(B)} = \sum_{B'} \Sigma^{(BB')}$ has been used for scalar and vector self-energies of the baryon B, and explicit dependence on all baryon densities has been dropped for notational simplicity. The finite density boundary conditions[7] are introduced through (2.5) and Dyson's equation

$$G_F^{(B)}(p) = S_F^{(B)}(p) + S_F^{(B)}(p)\Sigma^{(B)} G_F^{(B)}(p). \quad (3.15)$$

Denoting the excitation energy and effective mass for each baryon by

$$\mathscr{E}_B(\vec{p}) \equiv [p^2 + m_{e,B}^2]^{\frac{1}{2}} \quad (3.16)$$

$$m_{e,B} \equiv m_B + \Sigma_S^{(B)} , \quad (3.17)$$

the finite density baryon Green's functions are

$$G_F^{(B)}(p) = \frac{\gamma^0 [p_0 - \Sigma_V^{(B)}] - \vec{\gamma}\cdot\vec{p} - m_{e,B}}{2\mathscr{E}_B(\vec{p})} \left\{ \frac{1 - n_F^{(B)}(\vec{p})}{p^0 - \Sigma_V^{(B)} - \mathscr{E}_B(\vec{p}) + i\varepsilon} + \frac{n_F^{(B)}(\vec{p})}{p^0 - \Sigma_V^{(B)} - \mathscr{E}_B(\vec{p}) - i\varepsilon} - \frac{1}{p^0 - \Sigma_V^{(B)} + \mathscr{E}_B(\vec{p}) - i\varepsilon} \right\} . \quad (3.18)$$

The zero temperature distribution functions and the Fermi wave vector of the baryon B are defined according to

$$n_F^{(B)}(p) \equiv \theta(q_{F,B} - p) \quad (3.19)$$

$$q_{F,B}^3 \equiv 3\pi^2 N_B / V . \quad (3.20)$$

The total number of baryons in the system is given by

$$N = \sum_B N_B . \quad (3.21)$$

We observe that the three terms in the propagator (3.18) correspond to: (1) positive energy excitations above the filled Fermi sea; (2) positive energy excitations below the Fermi sea (holes); (3) and negative energy excitations. The ground state is devoid of physical anti-particles, although they may contribute through virtual states.

The baryon number and proper number densities $n^{(B)}$ and $\bar{n}^{(B)}$, defined by

$$n^{(B)} = \langle \psi_B^\dagger(x)\psi_B(x)\rangle = -i \lim_{x'\to x+0} \mathrm{tr}\{\gamma^0 G_F^{(B)}(x-x')\} , \quad (3.22)$$

and

$$\bar{n}^{(B)} = \langle \bar{\psi}_B(x)\psi_B(x)\rangle = -i \lim_{x'\to x+0} \mathrm{tr}\, G_F^{(B)}(x-x')$$

$$= -i \lim_{\eta\to 0} \int \frac{d^4p}{(2\pi)^4} e^{ip^0\eta} \mathrm{tr}\, G_F^{(B)}(p) , \quad (3.23)$$

are related to $\Sigma_V^{(B)}$ and $\Sigma_S^{(B)}$ through the $G_F^{(B)}$ as in (3.11) and (3.12):

$$\Sigma_V^{(BB')} = -\frac{g_V^2}{\mu_V^2} n^{(B')}, \tag{3.24}$$

and

$$\Sigma_S^{(BB')} = -\frac{g_S^2}{\mu_S^2} \bar{n}^{(B')}. \tag{3.25}$$

Through $\mathscr{E}_B(p)$ and $m_{e,B}$, as given in (3.16) - (3.17), the $\bar{n}$ and n are themselves functions of the Σ's.

In evaluating (3.11) and (3.12) we have dropped infinite terms which arise from the number density of filled negative energy states. The appearance of these terms is a direct consequence of the form of our lagrangian, and may be eliminated at the outset in either of two ways: (1) by normal ordering the lagrangian; or (2) by defining the physical number densities as the difference between n or $\bar{n}$ and the corresponding quantity at zero density. In either case we find the appropriate prescription in place of (3.11) or (3.12) is to replace the factor $e^{ip^0\eta}$ by $(e^{ip^0\eta}+e^{-ip^0\eta})/2$.

The solutions for the Green's functions will be complete if they are required to self-consistently reproduce the $n^{(B)}$ and $\bar{n}^{(B)}$. Using (3.18) in (3.22), it immediately follows that

$$n^{(B)} = q_{F,B}^3/3\pi^2 \tag{3.26}$$

This is identical to (3.20) and shows that the number density of *each species* is automatically self-consistent. Thus (3.22) is a trivial constraint and simply serves to define $q_{F,B}$. The proper number densities (3.23) lead to the consistency condition

$$\bar{n}^{(B)} = \int_0^{q_{F,B}} \frac{p^2 dp}{\pi^2} \frac{m_{e,B}}{\mathscr{E}_B(p)} = \frac{m_{e,B}}{2\pi^2}\left\{q_{F,B}\mathscr{E}_{F,B} - m_{e,B}^2 \ln\left|\frac{q_{F,B}+\mathscr{E}_{F,B}}{m_{e,B}}\right|\right\}. \tag{3.27}$$

To complete the solution we require that $\bar{n}^{(B)}$ (or equivalently $m_{e,B} = m_B - (g_S^2/\mu_S^2)\bar{n}^{(B)}$) be given by this transcendental algebraic equation. It is easily shown that in the low density limit ($q_F/m_B \to 0$) $m_{e,B}$ approaches m_B and $\bar{n}^{(B)}$ approaches $n^{(B)}$.

The consequences of (3.27) are significant: in the high density limit ($q_{F,B}/m_B \to \infty$) the number density $n^{(B)} \to \infty$. However, the only consistent solution of (3.27) in this limit is $m_{e,B} \to 0$. It will be observed that this does not occur in the absence of the self-consistency requirement,[12] since then $\bar{n}^{(B)}$ goes asymptotically as q_F^2. Because $\bar{n}^{(B)}$ is proportional to Σ_S and enters only as a correction to the physical mass, we may interpret (3.27) as a self-consistency conditon on the effective masses $m_{e,B}$.

For a system comprised of N different types of baryons there will be N conditions of the form (3.27). Each is an explicit function of one baryon mass $m_{e,B}$, and an implicit function of all others. Equations (3.27) therefore represent a set of coupled transcendental equations for the $m_{e,B}$. The relative simplicity of (3.27) is dependent on the fact that in this model both self-energies Σ_s^B and Σ_v^B are independent of external momentum. Generally speaking they could contain explicit dependence on the baryon four-momentum. The self-consistency conditions would then be replaced by a coupled set of transcendental integral equations whose solution would be extremely difficult, even by numerical means.

We conclude this section by emphasizing that the results above are fully relativistic, as regards both finite density and strong interaction effects, and treat the baryon physical degrees of freedom consistently throughout.

IV. Equations of State

The formal Green's function approach developed in the previous section will be used below to study the bulk properties of a system of superdense matter. To this end we review the physical information contained in the baryon Green's functions. We then fit the parameters of our model to nuclear matter.

A. Physical Information Contained in $G_F^{(B)}(p)$

Inspection of (3.18) shows that the excitation energies of the system as given by the poles of $G_F^{(B)}(p)$ are

$$\mathscr{E}_B(\vec{p}) = \Sigma_v^{(B)} + \sqrt{p^2 + m_{e,B}^2} \quad . \tag{4.1}$$

Since the self-energies are real, the excitations have an infinite lifetime, and represent eigenstates of the effective hamiltonian obtained from (3.3) treated in the Hartree approximation. In accordance with (2.13) the chemical potentials of the baryons are given by

$$\mu^{(B)} = \Sigma_v^{(B)} + \sqrt{q_{F,B}^2 + m_{e,B}^2} \quad . \tag{4.2}$$

The chemical potentials determine the equilibrium concentrations for the baryons in the system.

B. Bulk Properties Determined by $G_F^{(B)}(p)$

We have already discussed the number densities $n^{(B)}$ and

$\bar{n}^{(B)}$ as determined by (3.22) and (3.23). The chemical potential (4.2) and $n^{(B)}$ constitute N-2 of the N equations of state needed for a complete thermodynamic description of the system. Of the remaining two, the temperature is trivial: T = 0. The final equation of state is given by the pressure,

$$P = \sum_B \int_0^{q_{F,B}} n^{(B)} \frac{d\mu^{(B)}}{dq_{F,B}} dq_{F,B}$$

$$= -i \lim_{\eta \to 0^+} \sum_B \int d\mu^{(B)} \int \frac{d^4p}{(2\pi)^4} e^{ip^0\eta} \operatorname{tr}\{\gamma^0 G_F^{(B)}(p)\}. \quad (4.3a)$$

The summation includes only those baryons actually present in the system at a given density. Equation (4.3a) involves an integration over densities, through $\mu^{(B)}$, which is not always convenient. An alternate expression for P which involves integration over momenta follows from the stress energy tensor. As shown in Appendix A, the total baryon pressure is

$$P = \frac{1}{3} \langle \Phi_0 | \mathcal{T}^{ii} | \Phi_0 \rangle = \sum_B P^{(B)}$$

$$= -i \lim_{\eta \to 0^+} \int \frac{d^4p}{(2\pi)^4} e^{ip^0\eta} \sum_B \operatorname{tr}\{\tfrac{1}{3}\vec{\gamma}\cdot\vec{p} + \Sigma_S^{(B)} + \gamma^0 \Sigma_V^{(B)}\} \; G_F^{(B)}(p). \quad (4.3b)$$

When using (4.3b) the effective mass entering through $G_F^{(B)}$ and $\Sigma_S^{(B)}$ is constant so that the momentum integrals may be carried out analytically. Equation (4.3a) requires that $m_{e,B}$ be known for each value of $\mu^{(B)}$. The Green's function is given by (3.18), so that (4.3b) yields

$$P^{(B)} = 2\int \frac{d^3p}{(2\pi)^3} \frac{p^2}{\mathscr{E}_B(p)} n_F^{(B)}(p) + \frac{g_V^2}{\mu_V^2} n^{(B)} \int \frac{d^3p}{(2\pi)^3} n_F^{(B)}(p)$$

$$- \frac{g_S^2}{\mu_S^2} \bar{n}^{(B)} \int \frac{d^3p}{(2\pi)^3} \frac{m_{e,B}}{\mathscr{E}_B(p)} n_F^{(B)}(p)$$

$$= \frac{g_V^2}{2\mu_V^2} n^{(B)2} - \frac{g_S^2}{2\mu_S^2} \bar{n}^{(B)2} + \frac{1}{3\pi^2} \int_0^{q_F} \frac{p^4 dp}{\sqrt{p^2 + m_{e,B}^2}}$$

$$= \frac{1}{3}\left[\varepsilon^{(B)} - m_{e,B} \bar{n}^{(B)}\right] + \frac{g_V^2}{3\mu_V^2} n^{(B)2} - \frac{2}{3} \frac{g_S^2}{\mu_S^2} \bar{n}^{(B)2}, \quad (4.4)$$

where $\varepsilon^{(B)}$ is defined below. Equation (3.27) has been used to introduce the term $m_{e,B}\ \bar{n}^{(B)}/3$. A term corresponding to the infinite pressure of the filled negative energy states is included in (4.3b), but is easily removed by the method described in Section III. The result, equation (4.4), is finite.

All of the equations of state are now known, at least in principle, and the thermodynamic potentials could be found. However it is more direct to proceed with the Green's functions. The thermodynamic potential which we need to complete our analysis is the ground state energy density, which is just the

expectation value of the hamiltonian. We show in Appendix A that the ground state energy is given by

$$\varepsilon = \langle\Phi_0|\mathscr{H}|\Phi_0\rangle = \sum_B \varepsilon^{(B)} \tag{4.5a}$$

$$\varepsilon^{(B)} = -\frac{i}{2}\lim_{\eta\to 0^+}\int\frac{d^4p}{(2\pi)^4}\, e^{ip^0\eta}\, \mathrm{tr}\left[(\gamma^0 p_0 + \vec{\gamma}\cdot\vec{p} + m_B) G_F^{(B)}(p)\right]. \tag{4.5b}$$

In addition to the physically occupied positive energy states, the equations above contain contributions from all filled negative energy states, and these are removed as before. Notice that the physical mass m_B enters in the trace in (4.b).

The last equation may be applied directly to $G_F^{(B)}(p)$, and leads to

$$\varepsilon^{(B)} = \int\frac{d^3p}{(2\pi)^3}\frac{n_F^{(B)}(p)}{\mathscr{E}_B(\vec{p})}\{p^0[p^0 - \Sigma_v^{(B)}] + p^2 + m_B\, m_{e,B}\}$$

$$= \frac{q_{F,B}^3}{6\pi^2}\Sigma_v^{(B)} - \frac{m_{e,B}}{4\pi^2}\left\{q_{F,B}\mathscr{E}_{F,B} - m_{e,B}^2 \ln\left|\frac{q_{F,B}+\mathscr{E}_{F,B}}{m_{e,B}}\right|\right\}$$

$$+ \frac{1}{4\pi^2}\left\{q_{F,B}\mathscr{E}_{F,B}^3 - \tfrac{1}{2}m_{e,B}^2 q_{F,B}\mathscr{E}_{F,B} - \frac{m_{eB}^4}{2}\ln\left|\frac{q_{F,B}+\mathscr{E}_{F,B}}{m_{e,B}}\right|\right\}. \tag{4.6}$$

An alternate expression for the pressure, which follows from the first law of thermodynamics, uses the ground state energy density and is

$$P = n^2\frac{\partial(\varepsilon/n)}{\partial n}. \tag{4.7}$$

Finally consider the speed of sound v_s defined thermodynamically by the derivative at constant entropy

$$v_s^2 \equiv (\partial P/\partial\varepsilon)_s \tag{4.8}$$

for a system consisting of one baryonic species. Then P and ε are functions of q_F, and

$$v_s^2 = \left(\frac{\partial P}{\partial q_F}\right)_s \Big/ \left(\frac{\partial\varepsilon}{\partial q_F}\right)_s = \frac{n\, d\mu/dq_F}{\mu\, dn/dq_F}, \tag{4.9}$$

as follows from (4.3a) and the definition of the chemical potential $\mu \equiv (\partial\varepsilon/\partial n)_s$. Equations (4.2), (2.6), the self-consistency relation (3.27) for m_e, and straightforward algebra leads to the following expression for the adiabatic speed of sound:

$$v_s^2 = \frac{1}{3}\,\frac{q_F^2 + \frac{g_v^2}{\mu_v^2}\frac{q_F^3\mathscr{E}_F}{\pi^2} + \frac{g_s^2}{\mu_s^2}\frac{m_e^2 q_F^3}{\pi^2\mathscr{E}_F}\frac{A}{B}}{q_F^2 + m_e^2 + \frac{g_v^2}{\mu_v^2}\frac{q_F^3\mathscr{E}_F}{3\pi^2}} \tag{4.10}$$

$$A = 1 - \frac{m_e\mathscr{E}_F}{q_F^2}\ln\left|\frac{q_F+\mathscr{E}_F}{m_e}\right| \tag{4.11}$$

$$B = 1 + \frac{g_s^2}{\mu_s^2}\frac{m_e^3 q_F}{\pi^2 m_B\mathscr{E}_F}. \tag{4.12}$$

In the high density limit we find that A and $B \to 1$, and consequently

$$\lim_{q_F/m_B\to\infty} v_s^2 = 1. \tag{4.13}$$

Inspection of (4.13) shows that this is in fact just the asymptotic sound speed for a pure vector coupling $g_S = 0$. The scalar coupling ($g_V = 0$) would yield an asymptotic sound speed $v_s^2 \to 1/3$ equivalent to a relativistic free gas. It is notable that without the self-consistency imposed on m_e by (3.27), the scalar and the vector coupling would separately have the same limit (4.13). The limit (4.13) is significant since it shows that a consistent treatment based on Lorentz invariant nonlocal interactions at the lagrangian level automatically yields results consistent with macroscopic causality.

C. Nuclear Matter

Our model contains four quantities g_S, g_V, μ_S, μ_V which have yet to be specified. Inspection of (3.10) shows that these enter as the pairs g_V^2/μ_V^2 and g_S^2/μ_S^2 so that we actually are dealing with only two adjustable parameters. The model has a simple physical interpretation. If $\mu_S < \mu_V$ the scalar attraction will dominate at relatively low densities with the vector repulsion becoming important at higher densities. We fix the two parameters in our theory by requiring that a system with equal numbers of protons and neutrons be bound at nuclear densities ($q_{F,n} = q_{F,p} = 1.42\text{fm}^{-1}$) with binding energy $E_B = -15.75$ MeV per nucleon. Denote the total energy density by $\varepsilon = \varepsilon^n + \varepsilon^p$, the nucleon number density by $n = n^n + n^p$, and assume

a baryon mass $m_B = 939.0$MeV. Then (4.6) and

$$E_B = \frac{\varepsilon - nm_B}{n} \tag{4.14}$$

yield a binding energy of -15.74 MeV for $g_S^2/m_B^2/\mu_S^2\pi^2 = 27.04$ and $g_V^2 m_B^2/\mu_V^2\pi^2 = 19.83$. Our model is completely specified by the requirement that it satisfactorily describe nuclear matter. In this context we then realize that the intrinsic limits on this model stem from the uncertainties as to what constitutes nuclear matter. The sensitivity of the fit is discussed in Section VIII.

The energy density (4.6) for nucleons is identical with a result obtained by Walecka through an entirely different approach.[8] We remark that his fit to nuclear matter and ours are the same. A thorough comparison of the model's predicted properties (binding energy, effective mass, symmetry energy, etc.) with those obtained by other methods is given by Chin and Walecka.[13] As stressed there, agreement with phenomenological parameters is quite good.

It may appear surprising that a model as simple as one based on scalar and vector exchange should be in such close agreement with data on nuclear matter and nuclei. However, in view of our earlier remarks motivating the expansion in density we see that it should contain the essential physics of

superdense matter. Further refinements of the approximations are possible, but are not expected to have a dramatic effect on the equation of state, at least as regards normal Fermi fluids. With this groundwork for the development of the model, we feel that we are in a position to proceed to numerical values for superdense matter with the assurance that these results are firmly based on a strong theoretical relatively model independent foundation.

V. Bulk Properties of Superdense Matter

The results of the last section will be applied to determine the equations of state for the T = 0 system of leptons and baryons given in Table 1. This is accomplished in two stages. First, baryon chemical potentials are found from (4.2) and (3.27). Chemical equilibrium conditions then determine the densities at which each hyperon species appears in the system. Having found the constituents as a function of total baryon number density, we construct the ground state energy density and pressure equations of state from (4.7) and (4.6).

A. Composition of Superdense Matter

The particles given in Table 1 selected as the constituents for our model are the lowest mass spin ½ baryons known. Probably the only serious omission in this set is the Δ^-, which because of its low mass and negative charge would be expected to enter between the Λ^0 and Σ^0.[14] The inclusion of spin 3/2 particles would require straightforward but significant modification to the approach discussed here. An estimate of the effect of these missing constituents is given with our numerical results. Our equation of state yields matter at low densities $\varepsilon \lesssim 1. \times 10^7$ g/cm^3 which consists of nearly free protons and electrons. As the density increases it

becomes energetically favorable for protons to undergo e^- capture, with the simultaneous appearance of a non-zero density of neutrons. At higher densities these weak interactions result in hyperon production (hyperonization). The basic processes involved at $T = 0$ for an equilibrium ground state may be written as

$$B(e^-,\nu_e)B' \text{ and } B(\bar{\nu}_e,e^+)B' \qquad (5.1)$$

with B and B' suitably chosen members of the first baryon octet. Since the decays (5.1) are weak, the total electric charge Q and baryon number are conserved, and the change in charge and strangeness S of the baryons satisfies $\Delta S = \Delta Q$.

The chemical potentials of the constituent baryons determine the equilibrium composition. In this sense the μ's act as particle production thresholds. This has been thoroughly discussed in the literature.[15] The equilibrium conditions on the μ's which follow from (5.1) are given by Arbartsumyan.[16] Two dominant mechanisms determine the densities at which various baryons appear. The effective masses, which decrease with increasing density, tend to depress the threshold of each baryonic species. Due to the presence of e^- in the system, the chemical equilibrium conditions have the opposite effects on the positively charged baryons. Table 1 summarizes the order in which the baryons appear. The chemical potentials for individual species are shown in Figure 2. We

note that the interacting baryons enter in the same order as they would in a free hyperon gas. The number density of each species is shown in Figure 3 as a function of the total baryon number density, and the effective masses for selected baryons are shown in Figure 4.

B. Pressure and Energy Density

The ground state energy density is obtained from (4.6). A particular baryon will contribute a term $\varepsilon^{(B)}$ to the total ground state energy only when the number density n causes the chemical potential $\mu^{(B)}$ to exceed its production threshold. Once the total ground state energy density $\varepsilon = \sum_B \varepsilon^{(B)}$ has been found as a function of n, the pressure is obtained from (4.7) by numerical differentiation. Alternately (4.4) and the self-consistency condition (3.27) may be used. The first approach is numerically the simplest and has been followed here. Representative values of ε, P and n are presented in Table 2 and Figure 5. For energy densities $13.40 \leq \log \varepsilon \leq 14.11$ the slope of $P(\varepsilon)$ is negative, and for $13.64 \leq \log \varepsilon \leq 14.23$ the system pressure in negative. Throughout this density interval the system contains no hyperons. The dip in pressure indicates that the system possesses two different phases. The pressure P_c at which the phase transition occurs is determined by the usual Maxwell construction. P_c may be found by two equivalent means, as

illustrated in Figure 6, which shows P vs. $1/n_-$ and $\mu^{(n)}$ vs. P. In terms of the specific volume 1/n, P_c is determined by the requirement that the integrals $\int P\, d(1/n)$ from a to b and from b to c along the curve P(1/n) be equal (the region $P < 0$ is to be included). Alternately, P_c may be found as the point where the curve for the baryon chemical potential $\mu(P)$ intersects itself as shown in Figure 8b. For present purposes $\mu(P)$ may be replaced by $\mu^{(n)}(P)$ in determining P_c. Since the relative concentration of protons is small, this leads to negligible error.[17] We have calculated P_c both ways and find by each method $\log P_c = 30.336$. The phase transition occurs over the density range $3.44 \times 10^{12} < \varepsilon < 1.72 \times 10^{14}$ g/cm^3. The bulk modulus of the fluid in each phase is proportional to the slope of $P(\varepsilon)$. According to the standard convention the high density phase will be called a liquid while the lower phase will be called a gas. A detailed discussion of the ordering properties of the fluid in each of these phases is outside the scope of the present investigation. Therefore we will retain the simple classifications above for each fluid phase.

At low densities the equation of state approaches a free gas. The attractive interactions dominate above the transition region until $\varepsilon \simeq 1.82 \times 10^{14}$ g/cm^3, at which point

repulsive effects become significant. At higher densities repulsion dominates, and asymptotically $P \to \varepsilon$ as discussed previously. Hyperonization sets in at the Σ^- threshold, which occurs for $\varepsilon = 4.23 \times 10^{14}$ g/cm^3; the last hyperon in the octet appears when $\varepsilon \simeq 2.14 \times 10^{15}$ g/cm^3.

VI. Finite Temperature Corrections

Matter inside neutron stars will not be in its ground state during the initial formation process. Current evolutionary models suggest that the dense core will cool rapidly. Except for a short period following collapse the matter will be at nearly zero temperature.[18] It is therefore reasonable to assume that such systems will have temperatures satisfying $kT \ll \mu$ (where μ is the baryon chemical potential) when densities $\geq \epsilon_N$. We present below the lowest order temperature corrections to our model, restricting attention to a single component system. The inclusion of additional components offers no formal obstacles and may be achieved by a straightforward extension of the method discussed below. The expansions about $T = 0$ used below do not limit the relativistic nature of the interactions or the kinematics of the system. Our results therefore represent temperature corrections to a fully relativistic system.

The finite temperature of the system will be incorporated as boundary conditions on the fermion Green's functions which follow from the effective lagrangian (3.3). As a result of finite temperatures, fermions will not be restricted to their lowest possible energy states. Instead they will occur in the energy state p^0 with probability of occupancy given

by

$$n_F(p^0,\beta) = \frac{1}{e^{\beta(p^0-\mu)}+1} \quad . \tag{6.1}$$

The finite temperature Green's function for fermions is thus given by (2.5) with $n_F(p)$ replaced by (6.1).

This method of introducing boundary conditions is completely equivalent, at least for low temperatures, to the one employed by Bowers and Zimmerman in terms of the elementary lagrangian (2.1) and the Green's functions. The latter quantities contain suitably defined thermodynamic averages, a specific representation of which has already been discussed. The same thermodynamic averages for fermions are used here. The chemical potential μ entering through (6.1) is a function of temperature $T = (\beta k)^{-1}$ where k is Boltzmann's constant, and is determined by the number density through

$$n = 2\int \frac{d^3p}{(2\pi)^3} n_F(\vec{p},\beta). \tag{6.2}$$

The analysis of Section 4 is applicable to finite temperature systems if (6.1) is used. In particular the Green's function follows from (3.18) if $n_F(p)$ is replaced with (6.1). Note now that Σ_S and Σ_V will depend on β. Eqn. (3.22) now gives

$$n = 2\int \frac{d^3p}{(2\pi)^3} \{\exp \beta[\Sigma_V + \mathcal{E}(\vec{p},\beta) - \mu] + 1\}^{-1}, \tag{6.3}$$

while the proper number density is, from (3.23)

$$\bar{n}(\beta) = \frac{1}{(2\pi)^3}\int d^3p \, \frac{m_e(\beta)}{\mathcal{E}(\vec{p},\beta)} \left(\exp \beta[\Sigma_v + \mathcal{E}(\vec{p},\beta) - \mu] + 1\right)^{-1}, \quad (6.4)$$

where $m_e(\beta) = m_B - (g_s^2/\mu_s^2)\bar{n}(\beta)$ and m_B is the baryon physical mass. At $T = 0$ $m_e(\infty)$ and $\mathcal{E}(\vec{p},\infty)$ reduce to (3.16) - (3.17). The last equation represents the finite temperature self-consistency condition and reduces to (3.27) at $T = 0$. Equation (6.3) defines μ. Since the two self-energies Σ_v and Σ_s are each functions of n and $\bar{n}$, we see that the latter are now coupled.

In general integrals over $n_F(\vec{p},\beta)$ must be evaluated numerically. However we shall assume that $kT \ll \mu$ (semi-degeneracy), and expand about the $T = 0$ solutions.[19] If we make the change of variable $p = \sqrt{\mathcal{E}^2 - m_e^2}$ and define $x = \beta(\Sigma_v + \mathcal{E} - \mu)$ we obtain

$$n = \frac{1}{\beta^3\pi^2}\int_\alpha^\infty (x + \beta\mu - \beta\Sigma_v) \, \frac{\sqrt{(x+\beta\mu-\beta\Sigma_v)^2 - m_e^2\beta^2}}{e^x + 1}\, dx, \quad (6.5)$$

where $\alpha = \beta(m_e + \Sigma_v - \mu)$. We shall assume that $\alpha < 0$, as is true at $T = 0$. As long as this condition is satisfied, $\alpha \to -\infty$ as $T \to 0$, and n may be expanded about $T = 0$. Retaining

lowest order terms we find that

$$n = \frac{[(\mu-\Sigma_v)^2 - m_e^2]^{3/2}}{3\pi^2} + \frac{2(\mu-\Sigma_v)^2 - m_e^2}{6\sqrt{(\mu-\Sigma_v)^2 - m_e^2}}(kT)^2. \quad (6.6)$$

Proceeding in similar fashion, the proper number density may be expressed as

$$\bar{n} = \frac{m_e}{\pi^2\beta^2}\int_\alpha^\infty \frac{\sqrt{(x+\beta\mu-\beta\Sigma_v)^2 - \beta^2 m_e^2}}{e^x + 1}\, dx \quad (6.7)$$

which is, to lowest order in the temperature,

$$\bar{n} = \frac{m_e(\mu-\Sigma_v)}{2\pi^2}\sqrt{(\mu-\Sigma_v)^2 - m_e^2} - \frac{m_e^3}{2\pi^2}\ln\left|\frac{\mu-\Sigma_v+\sqrt{(\mu-\Sigma_v)^2-m_e^2}}{m_e}\right| + \frac{m_e(\mu-\Sigma_v)}{6\sqrt{(\mu-\Sigma_v)^2-m_e^2}}(kT)^2. \quad (6.8)$$

Although m_e and μ are functions of temperature, their $T = 0$ values are to be used in the last term of (6.7) and (6.8). The latter equations may be used to show that to lowest order in T,

$$\mu(\beta) = \mu(\infty) + A\beta^{-2} \quad (6.9)$$

$$m_e(\beta) = m_e(\infty) + B\beta^{-2}. \quad (6.10)$$

Substituting (6.9 - 6.10) into (6.6) and retaining lowest order terms leads to the following relation between A and B:

$$A = \frac{m_e}{\mathscr{E}_F} B - \frac{\pi^2(2q_F^2+m_e^2)}{6q_F^2\mathscr{E}_F} \quad . \tag{6.11}$$

We then substitute (6.9 - 6.10) into (6.8), use (6.11) to simplify the result and find, to lowest order in T,

$$B = \frac{(g_s^2/6\mu_s^2)m_e f(q_F)}{1+\frac{g_s^2}{2\pi^2\mu_s^2}\left(\mathscr{E}_F q_F + \frac{2m_e^2 q_F}{\mathscr{E}_F} - 3m_e^2 \ln\left|\frac{q_F+\mathscr{E}_F}{m_e}\right|\right)} \quad , \tag{6.12}$$

where

$$f(q_F) \equiv 1 + m_e^2/2q_F^2 \quad . \tag{6.13}$$

All quantities appearing in (6.11 - 6.13) are evaluated at T = 0, and are thus known.

The analysis above shows that the vector coupling does not effect the low temperature corrections to m_e or to μ. We also see that the temperature dependence of m_e results entirely from the scalar coupling, and that $m_e(\beta) = m_B$ if $g_s = 0$. When $g_s = 0$, $B = 0$ and (6.11) equals the coefficient of the lowest order temperature correction to the chemical potential of a free relativistic gas of fermions.[19] We thus see that the vector coupling has no effect on the chemical potential to lowest order in T.

Next consider the high density limit of B and A. Recalling that $m_e(\infty)\to 0$ and $\mu(\infty)\to q_F$, in this limit we find

$$\lim_{q_F/m_B\to\infty} m_e(\beta) = m_e(\infty)\left\{1 + \frac{\pi^2\beta^{-2}}{3q_F^2}\right\} \tag{6.14}$$

$$\lim_{q_F/m_B\to\infty} \mu(\beta) = \mu(\infty) - \frac{\pi^2\beta^{-2}}{3q_F} \quad . \tag{6.15}$$

For fixed q_F, finite temperature corrections tend to increase m_e, but the coefficient of β^{-2} tends to zero with increasing q_F. Equation (6.15) shows that the temperature dependence at high density is independent of the interactions; the latter enters only through $\mu(\infty)$.

Once m_e is known at T = 0, the coefficients A and B may be found at each value of q_F. Table 3 gives these for a system of neutrons in our model.

VII. Neutron Stars

The T=0 equations of state discussed in Section V have been used to construct model neutron stars. We present masses, radii and moments of inertia for slowly rotating neutron stars based on our model, and compare these with current models.

The method of constructing fully relativistic, slowly rotating neutron stars at zero temperature is well known. This procedure, including a detailed discussion of the numerical program, has been reviewed by Arnett and Bowers.[2] The essential steps are the following: Einstein's equations for a stationary axially symmetric rigidly rotating medium are expanded about the non-rotating solution.[20] The star's angular velocity is assumed to be $\Omega << \Omega_c = (MG/R^3)^{\frac{1}{2}}$. Expansions in (Ω/Ω_c) are obtained for the moment of inertia I, the gravitational mass M_G, and the mass $M_A \equiv m_A N$ where m_A is the atomic mass unit based on C^{12} and N is the proper baryon number.[21] To within limits set by the uncertainty in any recently constructed equations of state, including the present model, the corrections to M_G and M_A resulting from rotation are not significant, at least for values of the angular velocity Ω as presently observed in pulsars. For the pulsar in the crab nebula Ω_{crab} is approximately 200 sec^{-1}. The moment of inertia, however, does contain terms proportional to Ω/Ω_c which have been retained.

Model neutron stars based on other published equations of state have been surveyed.[2] The numerical structure program employed here is the same as that used by Arnett and Bowers. Thus our results may be compared directly with the other models as reported there.

In order to construct neutron star models an equation of state is needed which covers the density range $\varepsilon_s \leq \varepsilon < \varepsilon_{max}$, where ε_{max} is generally expected to be in the range 10^{15} - 10^{16}g/cm The surface density ε_s has been taken as $7.86 g/cm^3$ (the T=0 density of Fe^{56}). Our equation of state could be used throughout the density range above. However, the properties of low density cold catalyzed matter in neutron stars are well understood. According to current theories, as summarized in Table 4, the least reasonable equation of state at low densities is that of a gas. Therefore we patch to more nearly realistic low density models below the phase transition. Specifically, the results of Baym, Pethick and Sutherland[22] (BPS) have been used for $\varepsilon \leq 2.20 \times 10^{12}$ g/cm^3. For densities $\varepsilon > 1.72 \times 10^{14}$g/cm^3 our results have been used.

Selected neutron stars are given in Table 5. Each is parameterized by its central density ε_c. The mass M_G is shown in Figure 7 along with models based on the equations of state of Pandharipande[23] and Cameron, Cohen, Langer, and

Rosen (CCLR).[15] The latter treat the interactions non-relativistically. Figure 8 gives M_A as a function of ε_c for the same equations of state. The horizontal mark in Figure 7 gives M_G corresponding to $M_A = 1.41M_\odot$, and represents the mass of a supernova remnant favored by present evolutionary studies.[3,5] Stable neutron stars are those for which $dM/d\varepsilon_c > 0$ for both M_A and M_G. Configurations beyond the mass peak are gravitationally unstable and are expected to become black holes.[18]

The maximum stable mass at T=0 has, according to our model, a gravitational mass $M_G = 2.39M_\odot$ and $M_A = 2.89M_\odot$, and a central density $\varepsilon_c = 2.00 \times 10^{15}$ g/cm^3. This represents an increase of as much as 60% over values recently reported in the literature. If supernova remnants are in fact limited to masses M_A lying in a narrow range about $1.41M_\odot$, then the increased maximum mass is expected to have a dramatic effect on the predicted ratio of neutron stars to black holes produced by supernova. In essence our increased M_{max} implies that few black holes would be expected to result directly from the late evolutionary stages of isolated stars, and it may reduce the number of neutron stars in close binary systems which become black holes as a result of mass transfer.

Examination of M and R for models in Table 5 shows an interesting feature. As the mass decreases, the model radius R increases until the average density of the star falls below $\varepsilon \sim 8 \times 10^{14}$ g/cm^3. It then decreases with decreasing M until the average ε enters the phase transition region. For $\varepsilon \leq 2.2 \times 10^{12}$ g/cm^3 we again find that R increases as M decreases until the mass minimum is reached. The interval $dM/dR > 0$ corresponds to the region where the bulk modulus is large due to the steep slope of the P vs. ε curve. In fact the star distributes mass in this region as if it were nearly incompressible, the added matter primarily extending the surface while having a small effect on the central density.

Representative energy density profiles are shown in Figure 9. Also shown are mass fractions for selected models. Of the top three curves, the middle one corresponds to M_{max}. In these models more than 95% of the stellar matter is at densities greater than nuclear, corresponding to the highly incompressible fluid phase. For this reason the phase transition and the low density portions of $P(\varepsilon)$ have little effect on the structure. The density profiles are nearly flat out to $r = R$ and then drop nearly vertically to $\varepsilon = \varepsilon_s$. The lower three curves correspond to models which do feel the phase transition, and are sensitive to the equation of state at low densities. The

profiles are remarkably flat up to the phase transition, drop rapidly through this region, and then develop a low density envelope which balloons to large radii. The latter is due to the BPS equation of state. The sharp fall off in density makes it possible to clearly distinguish the inner core with $\epsilon \gtrsim 1.7 \times 10^{14} g/cm^3$ from the envelope for which $\epsilon \lesssim 2.2 \times 10^{12} g/cm^3$. The high density portion of the profiles are extremely flat out to the transition region, and account for nearly all of the mass of the star.

Moments of inertia have also been calculated for the neutron stars in Table 5. We find that the maximum moment of inertia occurs at ϵ_c of $1.5 \times 10^{15} g/cm^3$, and has the value $I_{max} = 3.13 \times 10^{45} g\text{-}cm^2$. Furthermore, stable models with masses in the range $M \gtrsim 1 M_\odot$ have moments of inertia greater than $10^{45} g\text{-}cm^2$. The maximum moment of inertia occurs at lower density than M_{max} as shown in Figure 10. Also shown are moments of inertia based on the non-relativistic equations of state of Pandharipande and of CCLR.

The two dashed horizontal lines in Figure 10 represent the region in which Trimble and Rees[24] place the lower bound on the moment of inertia for the pulsar in the crab nebula. Their estimate is based on the nebula's luminosity. Considerations of additional observational data[25] suggest that the lower

bound may approach $10^{45} g\text{-}cm^2$, in which case most neutron star models based on non-relativistic equations of state could be ruled out since they tend to yield $I_{max} < 10^{45} g\text{-}cm^2$. In fact the relatively high values of I for our model appear to be favored by estimates based on current observational data.

Our equation of state contains several features which bear directly on the internal structure of neutron stars. One is the clear distinction between the core and the crust. This follows from the essentially discontinuous change in density at the phase transition, which occurs over nearly two order of magnitude in density and at a pressure which corresponds closely with the pressure associated with neutron drip. In our model the phase transition is clearly identified with the formation of nuclear matter -- a highly incompressible fluid -- and therefore changes the usual mechanism for the smaller phase transition known as neutron drip. In our case the lattice of nuclear clusters is no longer viewed as vaporizing into a nucleon gas phase, but directly dissolving into the nuclear fluid as density increases. This direct, single transition from crystallized nuclear clusters into nuclear fluid provides a marked distinction between the low density matter in the envelope and the high density core. The development of an outer phase is thus a natural consequence of the

physics of the core. This modified picture of neutron star structure will have far ranging consequences for such phenomena as star quakes, couplings to magnetospheres, possible differential rotation rates, and the dynamic formation process itself.

Experience with neutron stars based on non-relativistic equations of state indicates that an increased maximum stable mass due to increased repulsion is associated with a reduction in core density. Associated with this is a tendency toward fewer hyperon species. In the CCLR model ($M_{max} = 2.45M_{\odot}$ and $\rho_c = 1.99 \times 10^{15} g/cm^3$) the only hyperons which actually contribute to the equation of state are the Σ^-, Λ^0 and Δ^-, the latter of which enters essentially at maximum mass . The remaining hyperons in the octet appear at significantly higher densities corresponding to unstable stellar equilibrium. Our equation of state shows nearly the same degree of repulsion as found in CCLR, and the maximum mass model occurs at practically the same density ($\varepsilon_c = 2. \times 10^{15} g/cm^3$). However all members of the octet, with the exception of the Ξ^0, contribute to the structure. This may be understood by examining the way in which the scalar and the vector interactions influence the equation of state and the particle thresholds. The relative stiffness of the

pressure-energy density curve is due almost entirely to the vector coupling, which dominates the scalar attraction above $\varepsilon = 2. \times 10^{14} g/cm^3$. The thresholds, however, are most strongly influenced by the self-consistency requirement which drives the heaviest baryon's m_e asymptotically to zero with increasing density ($m_{e,\Xi^-} \sim 400$ MeV when $\varepsilon \sim 2 \times 10^{15} g/cm^3$) as shown in Figure 6. This effectively increases the number of species that occur at a given density.

A complete analysis of the relation between observational data and the structural implications of this model are beyond the scope of this paper but will be reported elsewhere.

VIII. Conclusion

When the scalar and vector couplings were fitted in Section IV we observed that the greatest uncertainty in our model reflected that inherent in our description of nuclear matter. There we assumed E_B = -15.75MeV/baryon at a nuclear density parameterized by $q_{F,N} = 1.42 fm^{-1}$. However these values depend on the way in which the bulk properties of nuclei are extracted from experimental data. Values of E_B used in published models vary in the range $-15.3 > E_B > -16.5$[26] Quoted values of $q_{F,N}$ are equally uncertain.[27]

In order to test the sensitivity of our model we varied our values of E_B and $q_{F,N}$ by ±2% and redetermined g_S^2/μ_S^2 and g_V^2/μ_V^2. The variation in binding energy at fixed $q_{F,N}$ leaves the coupling constants unchanged to three significant figures. Thus to within the limits of currently accepted values these variations may be ignored. Variation in $q_{F,N}$ has a more significant effect on the equation of state. A 2% uncertainty shifts the value of the vector and scalar couplings by about 5%. We estimate that the neutron star stability limit will also change by about 2%, but in the direction opposite to $q_{F,N}$. Therefore the two percent uncertainty in $q_{F,N}$ implies approximately a $0.05M_\odot$ uncertainty in M_{max}.

We have included the baryons from the first SU(3) symmetric octet as possible constituents in our treatment of superdense matter. Threshold considerations show that the lowest mass pion-nucleon resonances should also be included. It is most likely that of these only the Δ^- and Δ^0 need to be considered. The former probably enters at about the same density as the Λ^0, while the Δ^0 would be expected to follow the Σ^0.[14] We have not included these resonances for two reasons: (1) kinematical complication associated with spin 3/2 propagators; (2) these couplings lead to phenomenological tensor meson exchange which would be difficult to determine from the physics of nuclear matter. We do not feel that a detailed treatment of these added constituents would greatly modify our general conclusions. For models with $\varepsilon_c < 5 \times 10^{14} g/cm^3$ the results of Section VII would remain unchanged. For models having higher central densities we can estimate the possible importance of the resonances by treating them as additional fermions in the system. Experience with neutron star models shows that the addition of a few extra fermion species results in a pressure decrease typically on the order of 10%.

Non-normal ground states such as superconductivity, superfluidity, pion condensation, ferromagnetism and crystal structure may play an important role in determining the properties

of superdense matter.[28] These effects may be incorporated in our approach by modifying the boundary conditions imposed on the Green's functions. It is probable that the first two have only a small influence on P and ε for static configurations, and thus should not produce substantial changes in our mass limit. Arguments based on non-relativistic models of normal superfluids scaled to the regime of nuclear densities imply[29] that if super effects do arise, the gap in the excitation spectrum should close when the density reaches 10^{15} g/cm^3. Since the maximum central density obtained in our model is 2×10^{15} g/cm^3, it is possible that these effects persist into the core. Because at least seven baryons enter at these densities, it may be possible that each contributes a super phase.

Pion condensation and related phenomena[30] are also interesting processes since the reactions $e^- \rightarrow \pi^- + \nu_e$ and $\mu^- \rightarrow \pi^- + \nu_\mu$ can occur at high densities and can carry off an impressive fraction of the star's energy. Physical π^- can be produced only when $\mu_e \approx \mu_{\pi^-}$. Using the physical value of the pion mass as the chemical potential of a T=0 condensed boson state μ_e would have to exceed 140MeV for production to occur. At all densities in our model $\mu_e < 125$MeV. However it should be clear from our results that there are possible interaction effects which could substantially reduce the pion effective

mass. The universal scalar meson coupling would have an effect on the π-meson propagators similar to that found in the case of the baryons. The baryon m_e's were decreased by about 800 MeV at densities on the order of 10^{15} g/cm^3. It is not difficult to imagine that the pion effective mass, even if coupled weakly, may be greatly reduced at similar densities. As this happens the e^- and μ^- decay modes shift towards pion production. Real π^- will then appear as a condensate, reducing the system pressure. Since this will only effect the lepton pressure, which is negligible compared to the baryon pressure, π^- condensates will not have a large direct effect on static neutron star structure. Table 6 summarizes the important physical parameters for selected neutron star models.

Another candidate for a physical realization of cold superdense matter is the strongly interacting particles. There are clear experimental indications that these hyperons are composed of a sea of objects which interact locally with an external current, have spin one-half, and obey statistics which are either Fermi or parafermi.[31] These objects, called quarks, carry with them the internal symmetries which are manifested by the strongly interacting particles. They are expected to be confined within the hyperons by interactions very similar to those which manifest themselves between the hyperons.

They are confined at energies and densities which are clearly relativistic. Furthermore, there are indications of phenomena in particle physics which require a many-body theory for their description.[32] It is therefore appropriate that we discuss the applicability of our approach to this problem. The study of superdense matter yields predictions which cannot be obtained from the study of systems comprised of only a few particles.

Only a slight modification of the formal approach which we have developed to treat superdense matter in neutron stars will be required in order to develop a preliminary model of the hyperons. In fact the results of Sections III and IV may be carried over directly to describe a simple quark model of the hyperons. In order to explore the feasibility of this approach we take as elementary constituents three quark species each having mass $m_Q = 6$ GeV.[33] We assume that each quark species couples with a universal scalar and vector coupling to baryon number, with strengths determined by our previous analysis. In treating the many-body aspect of the problem, the quarks are described by the usual Fermi many-body propagator (2.5) with m_B replaced by m_Q. The effect of parafermi statistics would lead only to a change in the degeneracy factor of order unity. Each type of quark is thus considered to have kinematic and collective properties similar to that of a massive spin 1/2 fermion. The model is now completely specified.

Proceeding as in Section IV we solved for the quark binding energy which reached its minimum value $E_B = -535$MeV for a quark number density $n = 7 \times 10^{39}\text{cm}^{-3}$. This is nearly forty times the number density for which the nuclear binding energy is a minimum. The quark effective masses $m_{e,Q}$ and the chemical potentials were found to have the same qualitative appearance as those of the baryons. The decrease in $m_{e,Q}$ is impressive, reaching a value $m_{e,Q}$ of 1100MeV at minimum binding energy. This effect alone could provide the explanation for the precocious scaling observed in the high energy phenomena.[34]

Finally we obtained the equation of state which is qualitatively similar to our hyperon equation of state. Further analysis, though, yields a Maxwell construction which occurs at a negative critical pressure. This is indicative of a system possessing a single condensed phase. It is possible that an analysis at finite temperature would produce two stable phases similar to our baryon results. The lower density phase would be identified as an interacting quark gas, and the high density phase, a fully condensed liquid, would be the only one surviving at $T = 0$. The minimum density for liquid quark matter in the model is $7.0 \times 10^{10}\text{g/cm}^3$.

In order to apply the model to hadronic matter it will be necessary to investigate these phases in detail. We have in mind a liquid droplet picture with the droplets being associated with baryons in equilibrium with a quark gas phase. The preliminary analysis above indicates that this simple picture is not consistent. The model indicates that a fully condensed fluid phase is the natural T = 0 state of a quark sea, and that cold droplets can be produced only by some additional formation mechanism. In other words, we find that quark confinement appears to be less difficult to explain than the formation process. However, if we construct a droplet of liquid quark matter at the minimum stable density and confine it to a volume derived from the proton Compton wavelength, the enclosed mass is 2.7×10^{-24}gm. It is remarkable that this corresponds roughly to a proton mass.

In order to obtain complete quark confinement within the droplets we would require additional physical mechanisms. One possible mechanism would utilize surface binding. It is notable that this is the mechanism of nuclei formation. Our model of nuclear matter is also found to possess only a liquid phase at zero temperature. A consistent description of atomic nuclei would then require the incorporation of additional formation mechanisms. A second and more interesting mechanism can

be inferred from our discussion of pion condensation in neutron stars. If the meson exchanges which are responsible for our fundamental interactions are also composed of quark constituents coupled universally to baryon number, these mesons will have their effective masses reduced significantly, possibly even to zero. In this context the vector meson octet could provide us with a candidate for a Yang-Mills non-abelian vector gauge field. This field would be the source of an infrared catastrophe, and could thus lead to complete confinement. A fuller treatment of the implications of our model of superdense matter to elementary particle physics will appear separately.

A final observation concerns the applicability of our approach to symmetry breaking effects and the masses of elementary particles. The formalism includes finite temperature effects, and may be used to study particle effective masses at high densities and high temperatures. In this regime it is possible that m_e approaches zero, and that a critical temperature exists below which specific masses "freeze out" to form a particle spectru . Examination of these problems will require additional development of the finite temperature effects on the meson propagators.

ACKNOWLEDGMENT

One of the authors (AMG) would like to thank the Aspen Center for Physics for providing an atmosphere for research in which some of this research took place.

APPENDIX A

The pressure and ground state energy density for a system of baryons may be expressed naturally in terms of Green's functions. The analysis could be carried out starting with (3.1) for $\mathcal{L}(x)$, and the Hartree approximation. The elimination of meson degrees of freedom can be performed at the end of the analysis. This procedure is unduly complicated for our present purposes. Instead consider the effective lagrangian density

$$\mathcal{L}(x) = \sum_B \bar{\psi}_B(x) \left\{ i\not{\partial} - m_B + \frac{1}{2} \sum_{B'} \left[\frac{g_s^2}{\mu_s^2} \bar{\psi}_{B'}(x)\, \psi_{B'}(x) - \frac{g_v^2}{\mu_v^2} \gamma^0\, \psi_{B'}^\dagger(x)\, \psi_{B'}(x) \right] \right\} \psi_B(x). \tag{A1}$$

The equations of motion for $\psi_B(x)$ are given by

$$\frac{\partial \mathcal{L}}{\partial \bar{\psi}_B} - \partial^\mu \frac{\partial \mathcal{L}}{\partial(\partial^\mu \bar{\psi}_B)} = 0 , \tag{A2}$$

and are

$$(i\not{\partial} - m_B)\psi_B(x) = -\sum_{B'} \left\{ \frac{g_s^2}{\mu_s^2} \bar{\psi}_{B'}(x)\, \psi_{B'}(x) - \frac{g_v^2}{\mu_v^2} \gamma^0\, \bar{\psi}_{B'}(x)\, \gamma^0\, \psi_{B'}(x) \right\} \psi_B(x) \tag{A3}$$

and its adjoint. The stress energy density tensor is

$$\mathcal{T}^{\mu\nu} = \sum_B \partial^\mu \psi_B(x) \frac{\partial \mathcal{L}}{\partial(\partial_\nu \psi_B(x))} - g^{\mu\nu}\, \mathcal{L}(x) . \tag{A4}$$

Using (A1) this becomes

$$\mathcal{T}^{\mu\nu}(x) = \sum_B \bar{\psi}_B(x)\, i\gamma^\nu \partial^\mu \psi_B(x) - g^{\mu\nu}\, \mathcal{L}(x). \tag{A5}$$

The hamiltonian density $\mathcal{H} \equiv \mathcal{T}^{00}$ follows immediately:

$$\begin{aligned} \mathcal{H}(x) &= \sum_B \bar{\psi}_B(x) \left\{ -i\vec{\gamma}\cdot\vec{\nabla} + m_B - \sum_{B'} \left\{ \frac{g_s^2}{2\mu_s^2} \bar{\psi}_{B'}(x)\, \psi_{B'}(x) - \left[\frac{g_v^2}{2\mu_v^2} \gamma^0\, \bar{\psi}_{B'}(x)\, \gamma^0\, \psi_{B'}(x) \right] \right\} \right\} \psi_B(x) \\ &= \sum_B \bar{\psi}_B(x) \{ -i\vec{\gamma}\cdot\vec{\nabla} + m_B - \sum_{B'} \frac{g_s^2}{2\mu_s^2} \bar{n}^{(B')} \\ &\quad + \sum_{B'} \frac{g_v^2}{2\mu_v^2} \gamma^0 n^{(B')} \} \psi_B(x) . \end{aligned} \tag{A6}$$

The last step corresponds to the Hartree approximation, in which $\bar{\psi}_B(x)\, \psi_B(x)$ and $\bar{\psi}_B(x)\, \gamma^0\, \psi_B(x)$ are replaced by $\bar{n}^{(B)}$ and $n^{(B)}$ respectively. The pressure P in a spherically symmetric and homogeneous system may be related to the expectation value of $\mathcal{T}^{\mu\nu}$ as follows:

$$\langle \mathcal{T}^{\mu\nu} \rangle = u^\mu u^\nu (P + \varepsilon) - g^{\mu\nu} P. \tag{A7}$$

Here u^μ is the velocity four-vector of a fluid element, and

ϵ is the ground state energy density. The thermodynamic average in (A7) is taken over the ground state

$$\epsilon = \langle \Phi_0 | \mathscr{T}^{00} | \Phi_0 \rangle = \langle \Phi_0 | \mathscr{H} | \Phi_0 \rangle . \tag{A8}$$

It follows from (A7) and (A8) that the total baryon pressure of the ground state is

$$P = \frac{1}{3} \sum_{i=1}^{3} \langle \Phi_0 | \mathscr{T}^{ii} | \Phi_0 \rangle \tag{A9}$$

$$\mathscr{T}^{ii} = \sum_B \bar{\psi}_B(x) \left\{ \frac{1}{3}[i\gamma^0 \partial_0 - m_B] + \sum_{B'} \left[\frac{g_s^2}{2\mu_s^2} \bar{n}^{(B')} - \frac{g_v^2}{2\mu_v^2} \gamma^0 n^{(B')} \right] \right\} \psi_B(x)$$

$$= \sum_B \bar{\psi}_B(x) \left\{ -\frac{i}{3} \vec{\gamma} \cdot \vec{\nabla} - \sum_{B'} \left[\frac{g_s^2}{2\mu_s^2} \bar{n}^{(B')} - \frac{g_v^2}{2\mu_v^2} n^{(B')} \gamma^0 \right] \right\} \psi_B(x). \tag{A10}$$

The last form follows from the equations of motion.

The definition of the baryon Green's function (2.3) is now used to rewrite the ground state averages of (A6) and (A9) in terms of $G_F^{(B)}(p)$. Consider the first term in (A6). Take the ground state average and rewrite it as follows

$$\langle \bar{\psi}_B(x)\, i\vec{\gamma} \cdot \vec{\nabla}\, \psi(x) \rangle = \lim_{x' \to x+0} i\vec{\gamma} \cdot \vec{\nabla}\, \langle \bar{\psi}_B(x')\, \psi_B(x) \rangle$$

$$= -\lim_{x' \to x+0} i\vec{\gamma} \cdot \vec{\nabla}\, \langle T\psi_B(x) \bar{\psi}_B(x') \rangle \tag{A11}$$

$$= -i \lim_{x' \to x+0} i\gamma^0 \frac{\partial}{\partial x_0} G_F^{(B)}(x - x').$$

The notation $x' \to x+0$ signifies that $x_0' = x_0 + \epsilon$ with ϵ a positive infinitesimal. The time ordering operator guarantees that the proper ordering $\bar{\psi}\psi$ will result. The same general procedure allows us to rewrite (A6) in terms of $G_F^{(B)}(x-x')$ to obtain

$$\epsilon = \langle \mathscr{H} \rangle$$

$$= -i \lim_{x' \to x+0} \mathrm{tr} \left[\sum_B \left(i\gamma^0 \frac{\partial}{\partial x_0} + i\vec{\gamma} \cdot \vec{\nabla} - m_B \right) G_F^{(B)}(x - x') \right.$$

$$\left. - \sum_{B'} \frac{g_s^2}{2\mu_s^2} \bar{n}^{(B')} + \sum_{B'} \frac{g_v^2}{2\mu_v^2} n^{(B')} \gamma^0 G_F^{(B)}(x - x') \right] . \tag{A12}$$

The equations of motion may be used to eliminate the interaction terms. If this is done we obtain

$$\epsilon = -\frac{i}{2} \lim_{x' \to x+0} \mathrm{tr} \left[\sum_B \left(i\gamma^0 \frac{\partial}{\partial x_0} + i\vec{\gamma} \cdot \vec{\nabla} + m_B \right) \right.$$

$$\left. - \frac{i}{2} \left(\frac{\partial}{\partial x_0} - \frac{\partial}{\partial x_0'} \right) \gamma^0 G_F^{(B)}(x - x') \right] . \tag{A13}$$

Substituting (3.18) for $G_F^{(B)}(x-x')$ into (A13) leads directly to the momentum space representation (4.5b). In this form all interaction effects enter through $G_F^{(B)}(p)$, and since the

integration is over baryon momentum the effective mass may be treated as a constant. We note that (4.5b) and the thermodynamic expression

$$\epsilon^{(B)} = \int \mu^{(B)} dn^{(B)} \qquad \text{(A14)}$$

yield similar integrals (one over $\vec{p}$ and the other over q_F). Both give identical results.

Proceeding in similar fashion for P we arrive at (4.3b). The details are straightforward and will not be reproduced here. As check the results above may be used to reproduce P and ϵ for a relativistic gas of non-interacting baryons.

FIGURE CAPTIONS

Figure 1: Typical low order irreducible self-energy diagrams resulting from (2.1) for exchange of vector, scalar or pseudoscalar particles (a-d). Leading order contributions to the expansion in density are given in (e).

Figure 2: Baryon chemical potentials in superdense matter vs. (total baryon number density)$^{1/3}$. Arrows on the abscissa indicate hyperon thresholds. The chemical potentials of all similarly charged baryons are equal. The chemical potential for Σ^- below threshold has not been shown.

Figure 3: Particle number densities vs. total baryon number density, both in cm^{-3}. The hyperon concentrations rise rapidly from zero once their thresholds are exceeded. The μ^- concentration drops to zero for $\log n_\mu \geq 38.6$. At higher densities there is a tendency for the n's to approach the same value. The actual threshold density for each hyperon is given in Table 1.

Figure 4: Representative baryon effective masses (MeV) vs. total baryon number density (cm^{-3}). To the scale

of the figure the effective mass of the nucleons are equal. The upper curve is for the Σ^-. Note that the baryon m_e's shift together. The physical rest masses are denoted on the ordinate. The arrow on the abscissa corresponds to nuclear density.

Figure 5: Equation of State: (a) Baym, Bethe, Pethick and Baym, Pethick, Sutherland equation of state; (b) results of this calculation; (c) free neutron gas. The horizontal line corresponding to log P = 30.34 represents the phase transition region. Curve b asymptotically approaches $P = \varepsilon c^2$.

Figure 6: Maxwell construction: (a) Schematic plot of total pressure P vs. 1/n. The dashed line represents the equation of state in the phase transition region. (b) Baryon chemical potential μ vs. pressure P. The thermodynamically realized state corresponds to the lowest value of μ. The transition pressure P_c is determined by the intersection of the μ curves for the liquid and gas phases.

Figure 7: M_G vs. ε_c for slowly rotating neutron stars. Curves a and b are described in Figure 5. Curve c represents the CCLR equation of state. The horizontal slashes indicate the mass M_G corresponding to a remnant mass $M_A = 1.41M_\odot$.

Figure 8: M_A vs. ε_c for slowly rotating neutron stars. The treatment follows Figure 7, except that the CCLR results have been omitted. The slash corresponds to $M_A = 1.41M_\odot$.

Figure 9: Energy density profiles for selected neutron star models (left scale). Note pronounced core for intermediate mass models. Three gravitational mass fraction curves are also shown (right scale). The arrow indicates the corresponding density profile. The extended envelopes are seen to contribute negligible mass to the system.

Figure 10: Moment of inertia vs. M_G. Treatment follows Figure 5. The (+) denotes the model with $M_A = 1.41M_\odot$. The range in the lower bound on I_{crab} is shown by the dashed lines.

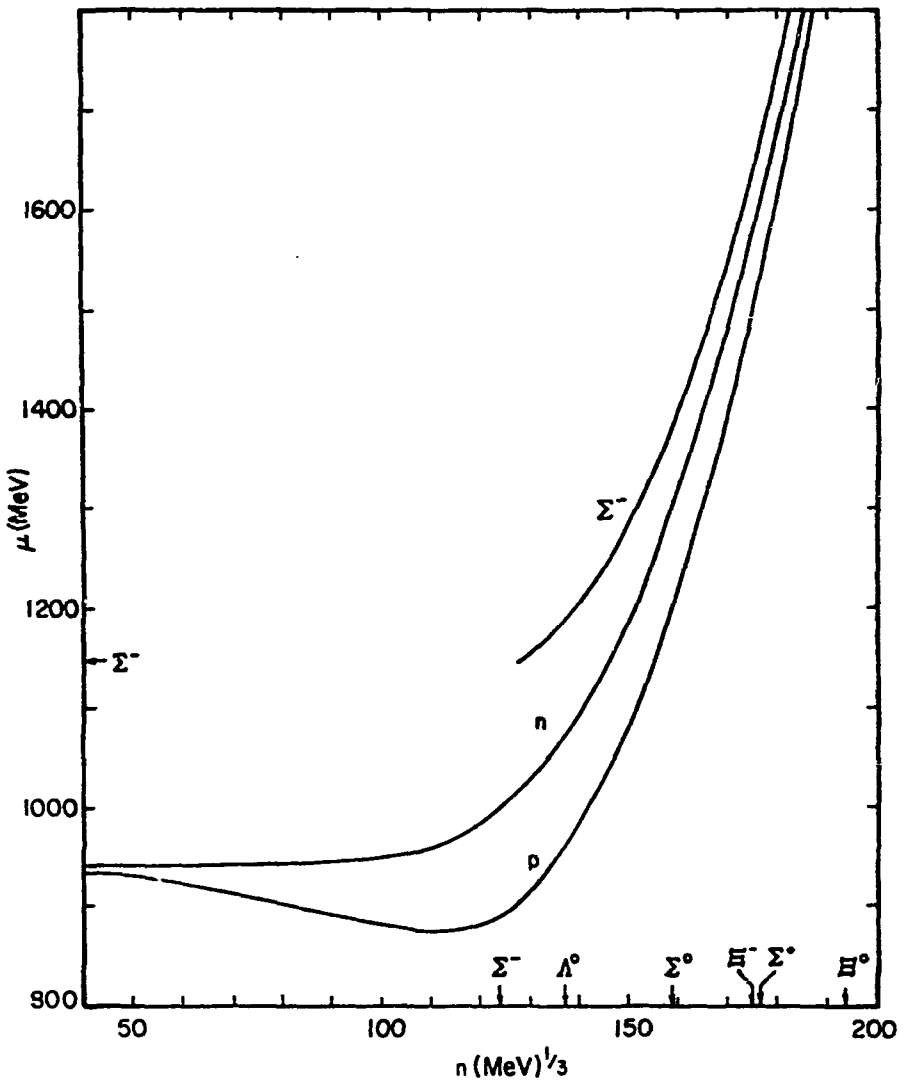

FIGURE 2

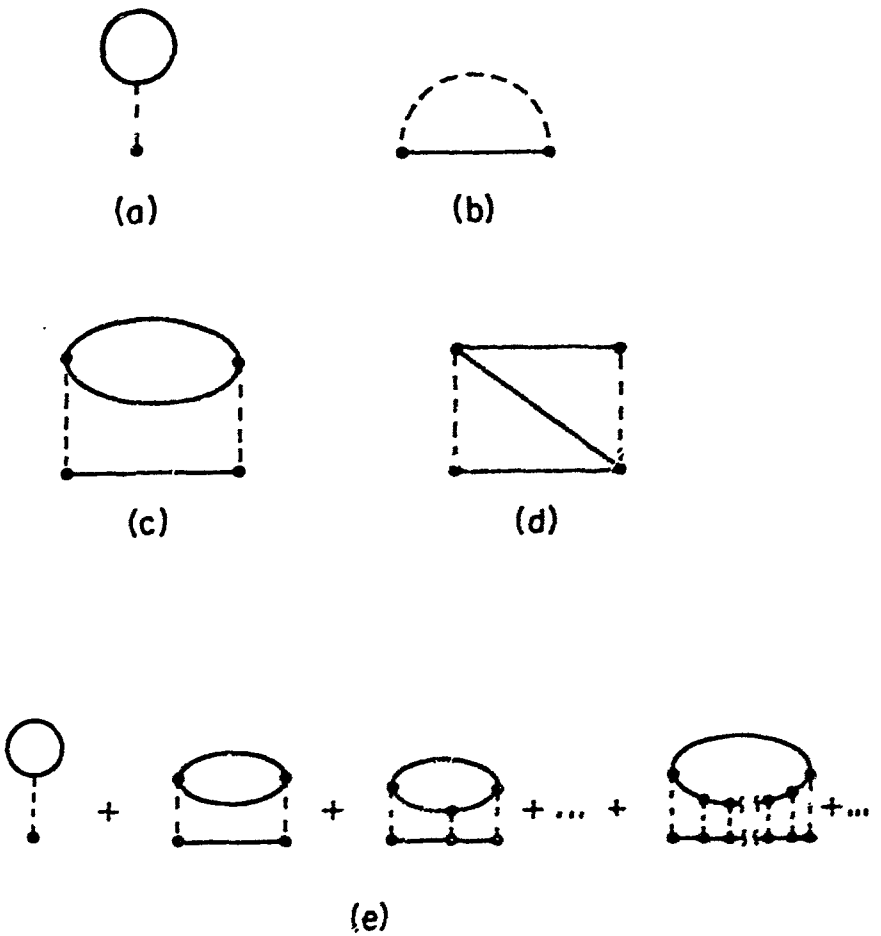

FIGURE 1

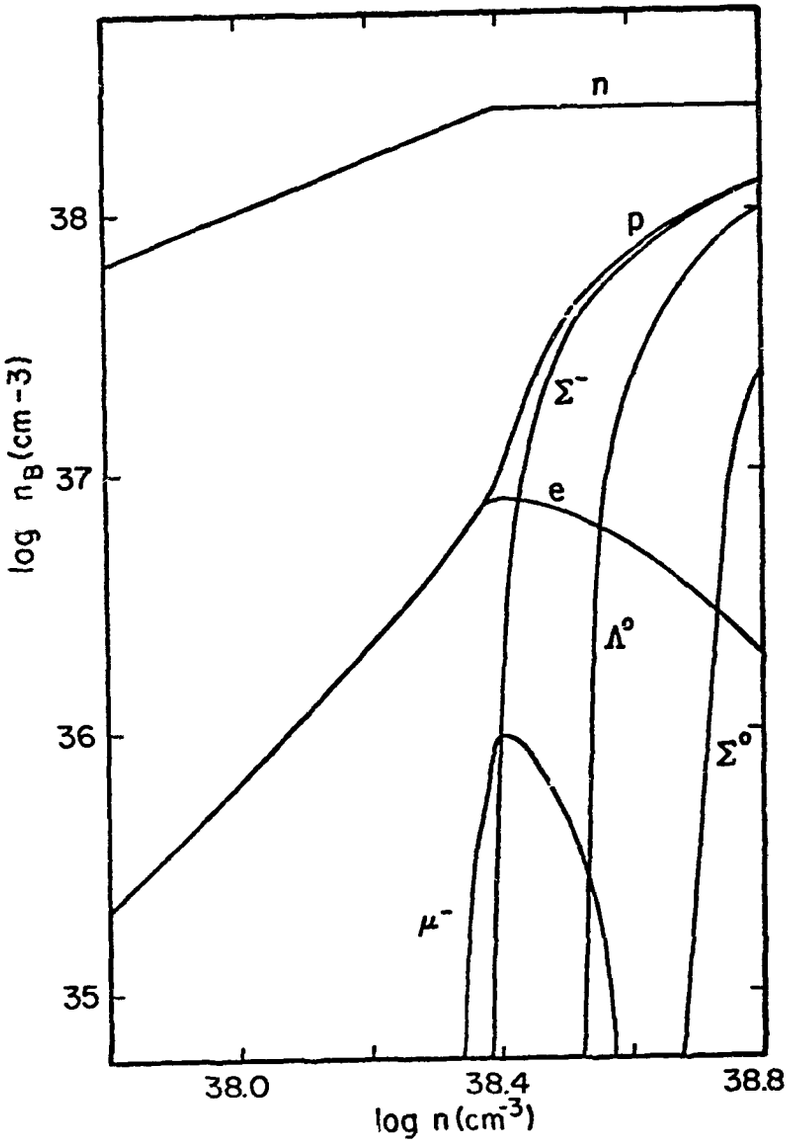

FIGURE 3

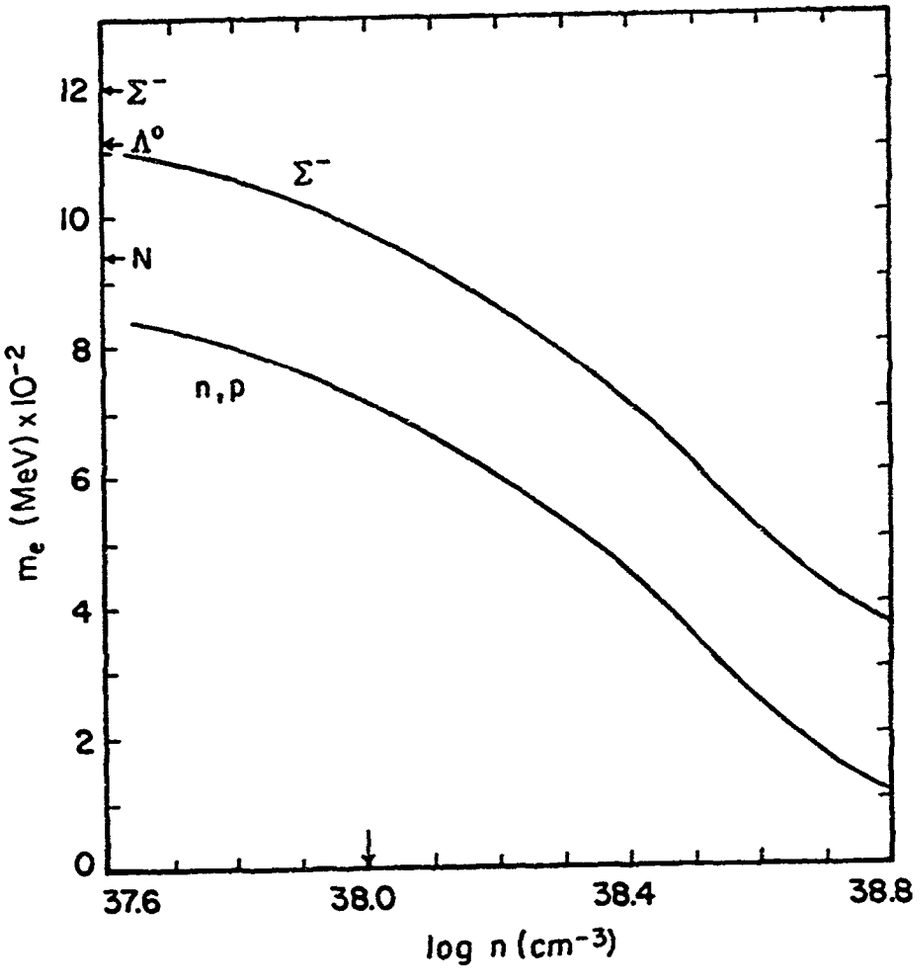

FIGURE 4

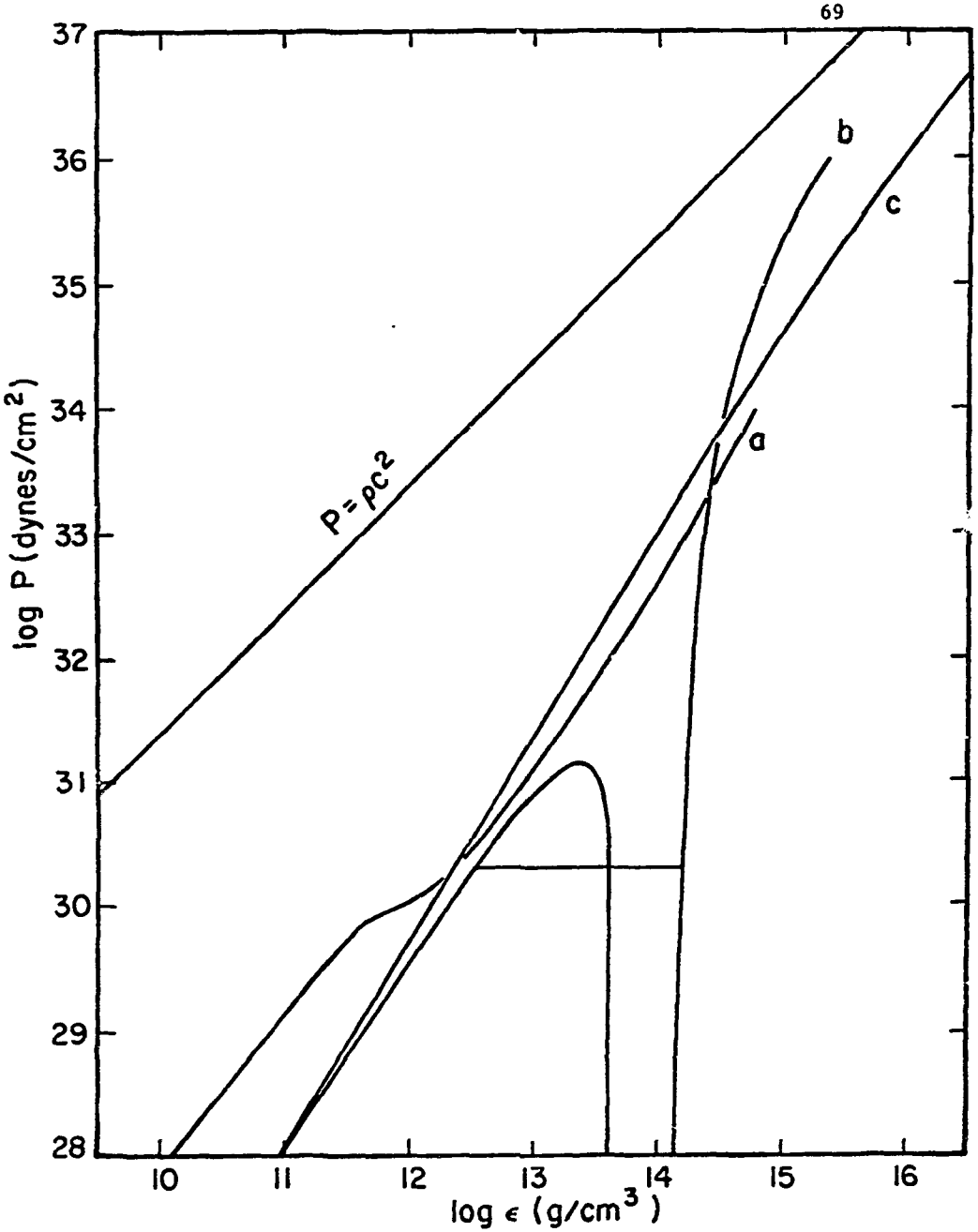

FIGURE 5

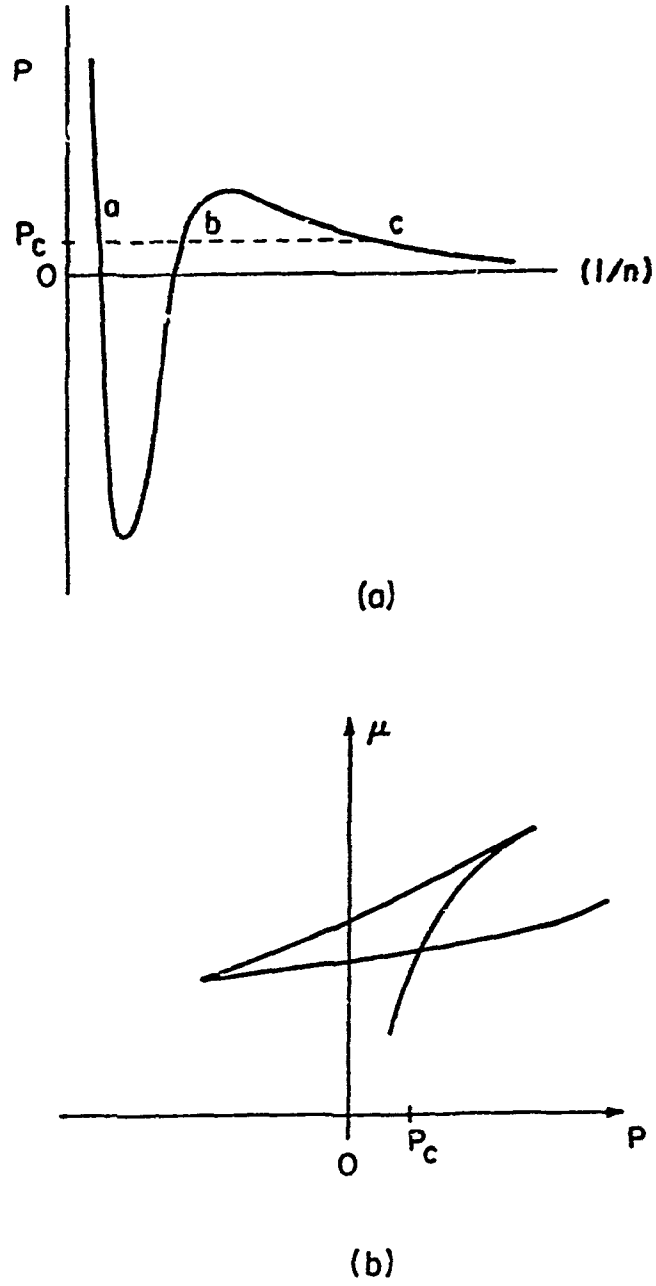

FIGURE 6

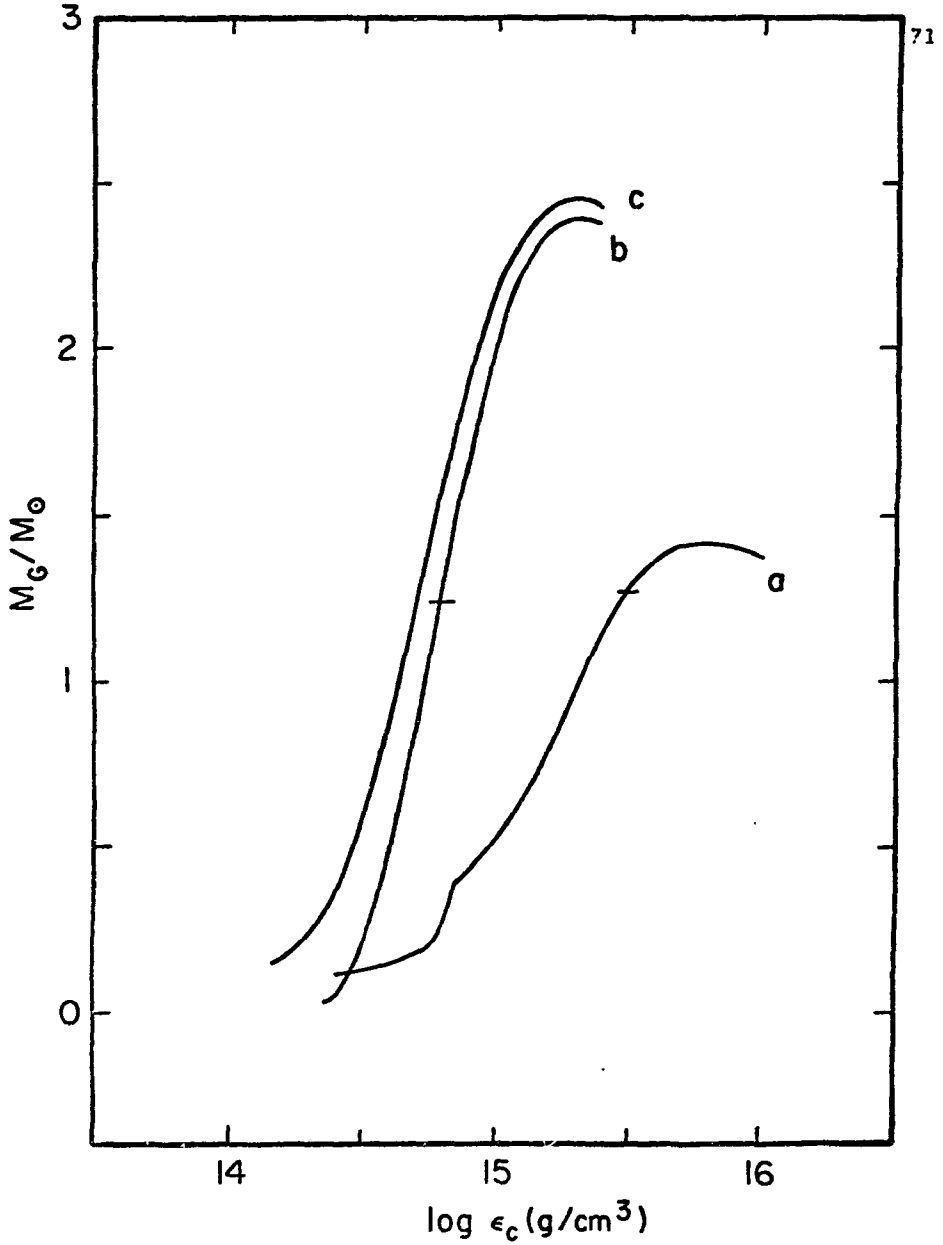

FIGURE 7

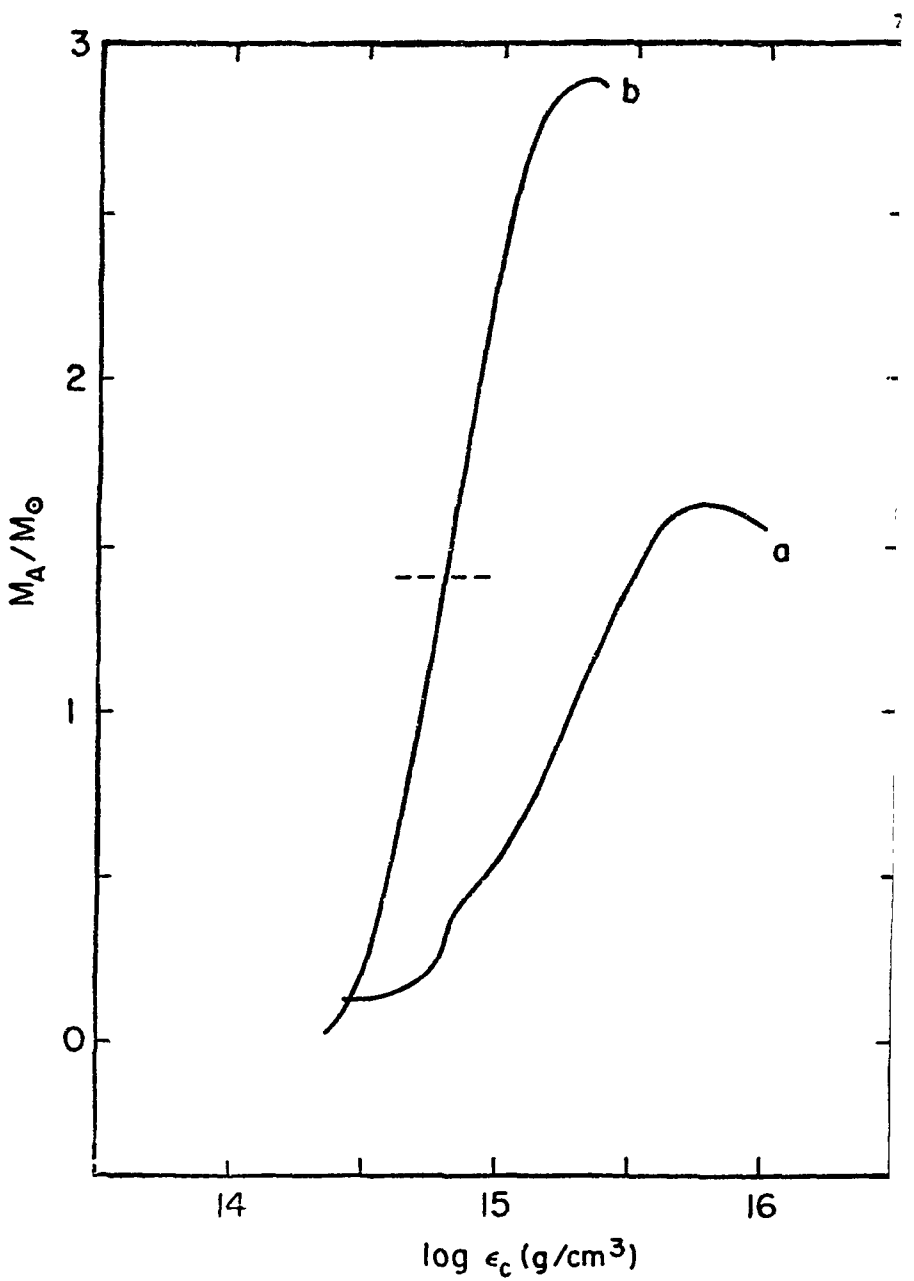

FIGURE 8

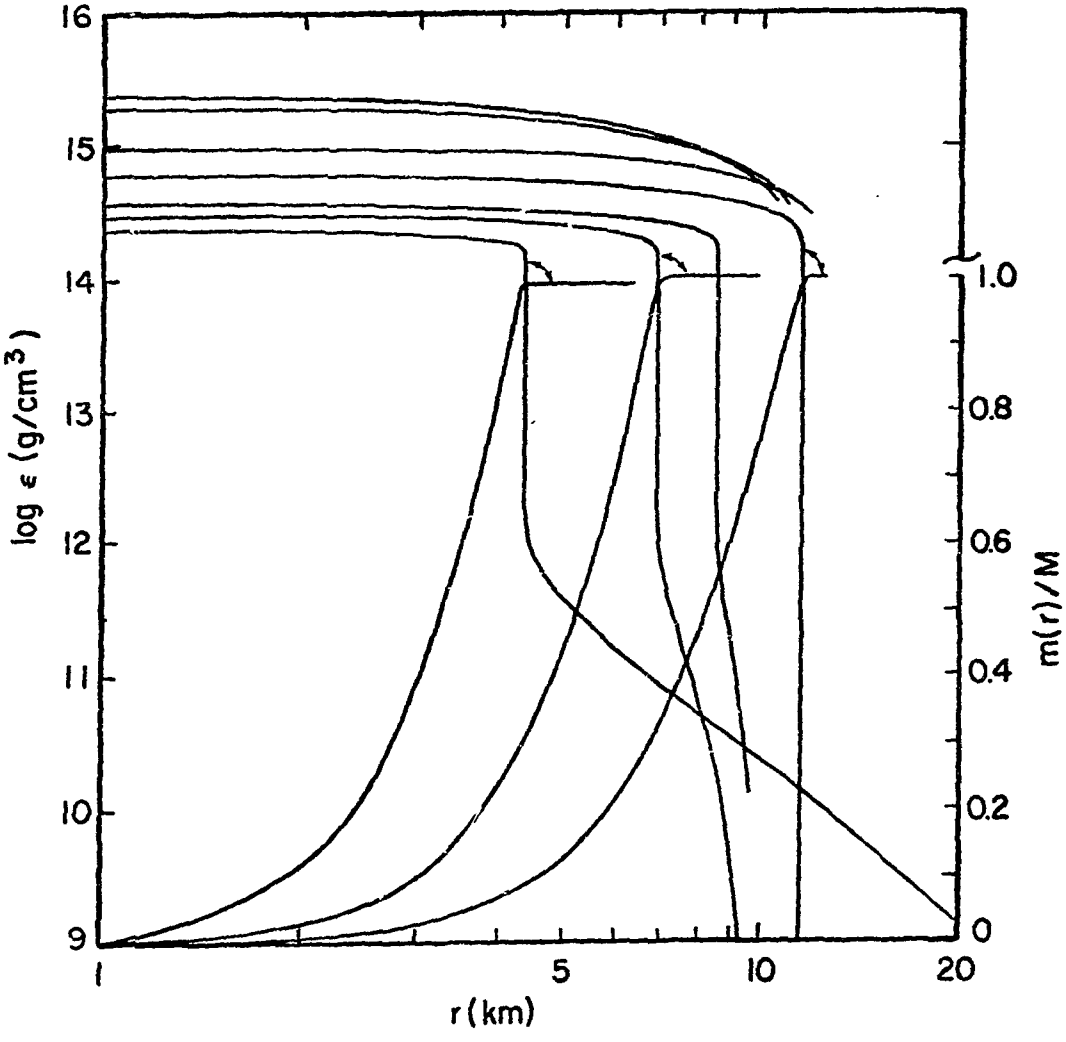

FIGURE 9

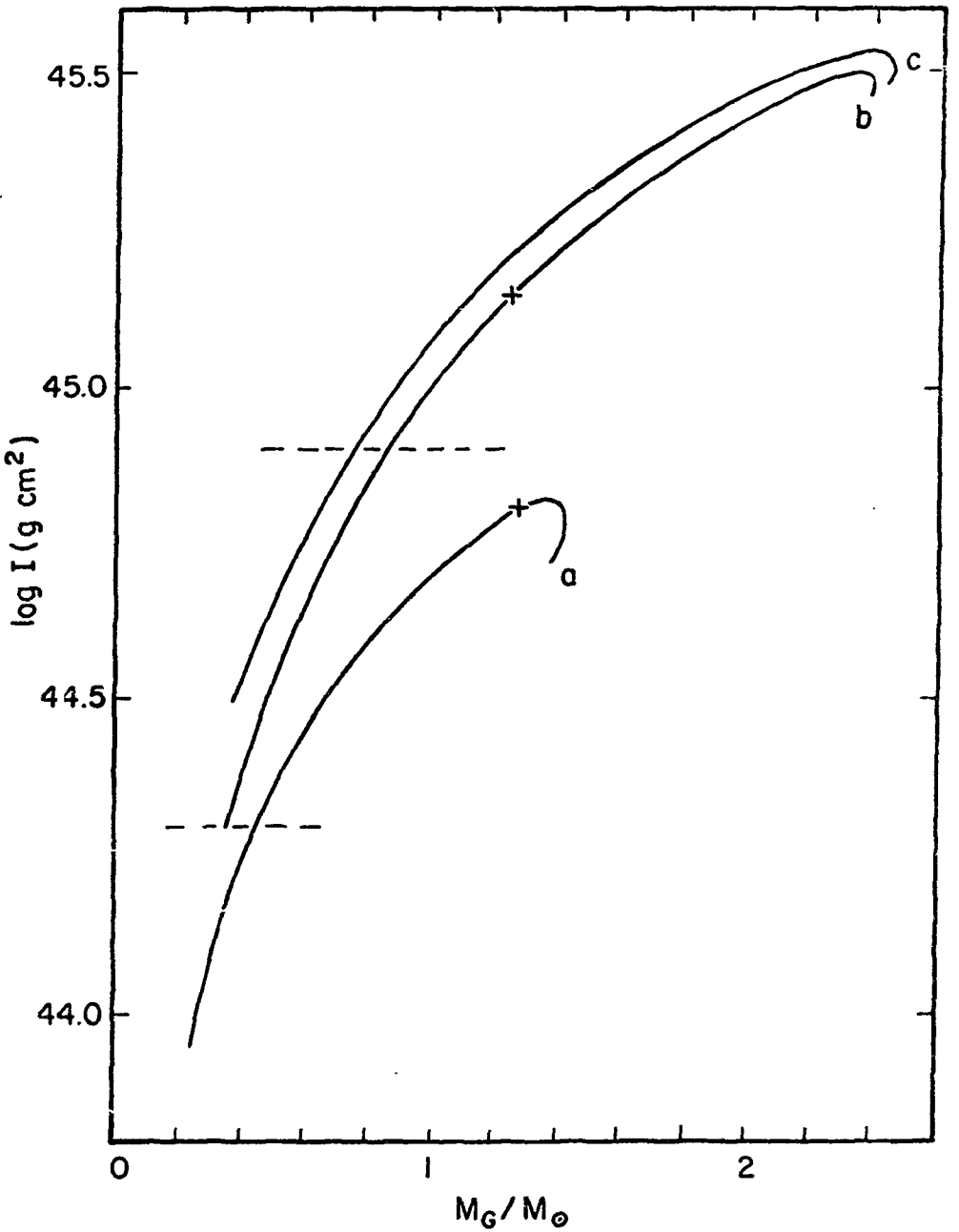

FIGURE 10

TABLE CAPTIONS

Table 1: Particle thresholds. The columns give: (1) particle; (2) rest mass in MeV; (3) total baryon number density (cm^{-3}) for which particle appears in the interacting system; (4) same as (3) for free particles; (5) threshold in total baryon energy density (g/cm^3). The proton (m_p = 938.3 MeV) and electron (m_{e^-} = 0.511 MeV) are present from zero density.

Table 2: Equation of State. The first three columns give the baryon energy density $\varepsilon(g/cm^3)$, pressure $P(dynes/cm^2)$ and total number density $n(cm^{-3})$. The last three columns give the proton, neutron and Σ^- chemical potentials (MeV) in the system. Several entries are given in the region of the phase transition; these values of the pressure, indicated by *, were replaced by 2.165E30 for the present calculation.

Table 3: Temperature corrections to m_e and μ for neutrons. The coefficients A and B appearing in (8.9 - 8.10) as well as μ for pure neutrons are given.

Table 4: Composition of cold matter as expected for neutron stars.

Table 5: Slowly rotating neutron stars. The columns give: (a) central density (g/cm^3); (b) gravitational mass in solar units ($M_\odot = 1.987 \times 10^{33}$g); (c) mass M_A in solar units (see Section VII); (d) radius (km); (e) moment of inertia ($g\text{-}cm^2$); (f) binding energy per baryon (MeV/baryon). The notation E15 means $\times 10^{15}$, etc.

Table 6: Summary of neutron star structure. The three models listed are: (a) critical model representing the most massive stable neutron star; (b) the model having maximum moment of inertia; (c) model whose "remnant" mass $M_A = 1.41 M_\odot$.

TABLE 1

Particle	Rest Mass (MeV)	$n \times 10^{-39}$ (cm^{-3})		$\varepsilon \times 10^{-15}$ (g/cm^3)
		Interacting	Free	Interacting
n	939.6	$\approx 10^{-8}$	$\approx 10^{-8}$	$\approx 10^{-8}$
μ^-	105.7	0.213	0.462	0.369
Σ^-	1197.4	0.245	0.617	0.423
Λ^0	1115.6	0.327	1.22	0.577
Σ^0	1192.5	0.511	3.33	0.950
Ξ^-	1321.3	0.697	3.91	1.43
Σ^+	1189.4	0.712	>6.8	1.48
Ξ^0	1314.9	0.951	>6.8	2.14

TABLE 2

ε (g/cm^3)	P ($dynes/cm^2$)	n (cm^{-3})	μ^p (MeV)	μ^n (MeV)	μ^{Σ^-} (MeV)
2.340E11	3.810E28	1.396E35	938.2	940.0	...
4.755E11	1.159E29	2.837E35	938.1	940.3	...
1.113E12	4.251E29	6.637E35	937.9	940.7	...
1.914E12	9.465E29	1.142E36	937.6	941.0	...
3.443E12	2.165E30	2.053E36	937.0	941.5	...
6.681E12	5.107E30*	3.981E36	935.9	942.2	...
1.265E13	1.014E31*	7.533E36	933.7	942.7	...
2.305E13	1.431E31*	1.372E37	930.1	943.0	...
3.542E13	9.347E30*	2.108E37	925.9	942.8	...
4.335E13	4.798E29*	2.580E37	923.2	942.6	...
6.688E13	-4.673E31*	3.981E37	915.6	941.7	...
1.695E14	-2.086E31*	1.010E38	887.9	941.4	...
1.723E14	2.818E30	1.027E38	887.3	941.5	...
1.732E14	1.132E31	1.032E38	887.1	941.6	...
1.760E14	3.790E31	1.049E38	886.5	941.7	...
1.825E14	1.088E32	1.088E38	885.2	942.2	...
1.972E14	3.216E32	1.175E38	882.4	943.4	...
2.272E14	1.027E33	1.354E38	877.7	946.9	...
2.730E14	3.036E33	1.625E38	873.4	955.4	...
2.996E14	4.868E33	1.781E38	872.7	962.3	...
3.530E14	1.041E34	2.091E38	875.8	980.4	...
4.184E14	2.102E34	2.464E38	888.8	1010.	1131.
5.261E14	3.790E34	3.051E38	930.2	1048.	1165.
6.621E14	7.290E34	3.757E38	1003.	1111.	1220.
8.021E14	1.264E35	4.438E38	1094.	1193.	1292.
1.044E15	2.514E35	5.507E38	1264.	1349.	1434.
1.146E15	3.102E35	5.919E38	1333.	1413.	1493.
1.333E15	4.265E35	6.633E38	1456.	1529.	1601.
1.617E15	6.137E35	7.623E38	1650.	1693.	1756.
1.966E15	8.520E35	8.719E38	1820.	1875.	1930.
2.119E15	1.177E36	1.000E39	2044.	2091.	2139.

TABLE 3

$q_{F,N}$(fm-1)	v_N(MeV)	A(MeV^{-1})	B(MeV^{-1})
0.05680	939.7	1.541E+2	1.664E+2
0.1420	940.0	2.466E+1	2.664E+1
0.2272	940.4	9.630E0	1.041E+1
0.3124	941.0	5.084E0	5.504E0
0.4260	941.8	2.715E0	2.947E0
0.5680	942.6	1.499E0	1.635E0
0.7100	943.0	9.272E-1	1.018E0
0.8520	942.9	6.095E-1	6.758E-1
0.9940	942.2	4.129E-1	4.642E-1
1.136	941.2	2.822E-1	3.234E-1
1.278	940.5	1.910E-1	2.252E-1
1.420	941.4	1.259E-1	1.547E-1
1.562	946.1	7.915E-2	1.038E-1
1.704	958.8	4.616E-2	6.739E-2
1.846	985.9	2.386E-2	4.216E-2
1.988	1035.	9.885E-3	2.560E-2
2.130	1113.	1.997E-3	1.546E-2
2.272	1220.	-2.017E-3	9.596E-3
2.414	1355.	-3.911E-3	6.256E-3
2.556	1516.	-4.749E-3	4.300E-3
2.698	1701.	-5.077E-3	3.100E-3
2.840	1908.	-5.154E-3	2.323E-3

TABLE 4

ρ(g/cm^3)	Composition
10^4 - 7×10^6	Normal nuclei and non-relativistic e^-
7×10^6 - 4×10^{11}	Relativistic e^- and Coulomb lattice of increasingly neutron rich nuclei
4×10^{11} - 2×10^{14}	Neutron drip; accumulation of free neutrons and nuclear clusters
$> 2 \times 10^{14}$	Clusters dissolve; n, p, and e^- Fermi fluids
$> 3 \times 10^{14}$	Hyperonization

TABLE 5

Neutron Star Models					
ϵ_c (g/cm^3)	$M_G/M_\odot$	$M_A/M_\odot$	R(km)	I ($g\text{-}cm^2$)	ϵ_B (MeV/baryon)
2.000E15	2.39	2.89	11.42	3.05E45	172.0
1.500E15	2.33	2.81	11.89	3.13E45	167.1
1.259E15	2.24	2.68	12.14	3.05E45	159.3
1.000E15	2.02	2.36	12.37	2.70E45	142.2
8.000E14	1.68	1.91	12.40	2.12E45	118.8
7.499E14	1.57	1.76	12.36	1.92E45	111.2
6.402E14	1.28	1.41	12.16	1.45E45	94.1
6.310E14	1.26	1.38	12.14	1.41E45	91.5
5.623E14	1.06	1.15	11.90	1.10E45	79.2
4.000E14	0.540	0.564	10.78	3.93E44	45.8

TABLE 6

	$M/M_\odot$	R(km)	$I \times 10^{-45}$
Critical model	2.38	11.42	3.05
Maximum moment of inertia	2.33	11.89	3.13
Remnant model ($M_A = 1.41M_\odot$)	1.28	12.16	1.45

FOOTNOTES AND REFERENCES

1. An excellent review of previous work on this subject may be found in V. Canuto, "Equations of State at Ultra High Densities", Ann. Rev. Astron. Astrophys. (to be published).
2. W. D. Arnett and R. L. Bowers, Publications in Astronomy, No. 9, The University of Texas at Austin, July 1974.
3. W. D. Arnett, Ap. J. 195, 727 (1975).
4. G. Borner and J. M. Cohen, Ap. J. 185, 959 (1973).
5. W. D. Arnett, Ap. J. 194, 373 (1974).
6. The notation pertinent to relativistic fields and Green's functions follows that given in J. D. Bjorken and S. D. Drell, "Relativistic Quantum Fields" (McGraw-Hill, New York, 1965).
7. R. L. Bowers and R. L. Zimmerman, Phys. Rev. D7, 2289 (1973); R. L. Bowers, J. A. Campbell and R. L. Zimmerman, Phys. Rev. D7, 2278 (1973); and D7, 296 (1973).
8. J. D. Walecka, Ann. Phys. (N.Y.) 83, 491 (1974).
9. A discussion of the procedure leading to this type of result is given in Ref. 7.
10. R. L. Bowers, D. Pedigo, A. M. Gleeson, and R. L. Zimmerman, to appear in the Astrophysical Journal.
11. In addition these fields will not be associated with any of the observed physical particles.

12. This has been discussed for a scalar coupling in a different approach by Kalman, Phys. Rev. D9, 1656 (1974).
13. S. A. Chin and J. D. Walecka, Phys. Letters 52B, 24 (1974).
14. This estimate is based on chemical equilibrium of non-interacting baryons, but it is also consistent with the results of a non-relativistic models which includes interactions.
15. J. M. Cohen, W. D. Langer, L. C. Rosen and A. G. W. Cameron, Astrophys. and Space Science 6, 228 (1970).
16. V. A. Ambartsumyan, Sov. Astron. AJ, 37, 193 (1960).
17. As seen from Figure 3 $n^{(p)}$ is more than two orders of magnitude less than $n^{(n)}$ for densities in the vicinity of the phase transition.
18. Ya. B. Zel'dovich and I. D. Novikov, Stars and Relativity, University of Chicago Press (1971).
19. A detailed discussion of finite temperature corrections is given in H. Y. Chiu, Stellar Physics, Blaisdell Publ. Co. (1968).
20. J. B. Hartle, Ap. J. 150, 1005 (1967).
21. The masses are discussed in Refs. 2 and 18.
22. G. Baym, C. Pethick, and P. Sutherland, Ap. J. 170, 299 (1971).
23. V. Pandharipande, Nucl. Phys. A178, 123 (1971); A174, 641 (1971).

24. V. Trimble and M. Rees, Astrophys. Letters 5, 93 (1970).

25. G. Borner and J. M. Cohen, Ap. J. 185, 959 (1973).

26. W. D. Meyers and W. J. Swiatecki, Nucl. Phys. 81, 1 (1966); P. A. Seeger and W. M. Howard, Los Alamos Scientific Laboratory Report LA-5750, Oct. 1974.

27. L. R. B. Elton, Nuclear Sizes, Oxford University Press, London (1961); J. W. Negele, Phys. Rev. 61, 1260 (1970); H. A. Bethe, Annual Rev. of Nuclear Sci. 21, 93 (1971).

28. K. J. Hansen, ed., "Physics of Dense Matter", IAU Symposium No. 53, Boulder, Colorado, August 1972.

29. V. L. Ginzburg, Sov. Phys. Usp., 12, 241 (1969).

30. R. Sawyer, Phys. Rev. Letters, 29, 382 (1972); A. B. Migdal, Phys. Rev. Letters, 31, 257 (1973).

31. There is a vast literature in which these ideas are given and surveyed. Since we cannot list even partially the principle references we list here some recent review articles. F. Gilman in Proceeding of the SLAC Summer Institute, 1974 (to be published); R. P. Feynman, Summary talk given at International Conference on Neutrino Physics and Astrophysics Philo. April 1974; The John's Hopkins University Workshop on Current Problems in High Energy Particle Theory, Ed. by G. Domokos and S. Kövesi-Domokos (1974).

32. E. L. Feinberg, Physics Reports 5, 237 (1972) and references contained therein.

33. The quark mass is as yet undetermined but there are indications that it must be at least this large. J. Kokkedee, "The Quark Model", W. J. Benjamin, Inc. (1969); Y. S. Kim and N. Kwak, "Fields and Quanta" 5, 1 (1972).

34. R. Slansky, Physics Reports 11c, 99 (1974) and references contained therein.